

Nanoplankton dominate autumn biomass on the Agulhas Bank

Sixolile Leonora Mazwane¹, Alex James Poulton², Margaux Noyon³, Emma Rocke⁴, and Michael John Roberts¹

¹Nelson Mandela University

²Lyell Centre for Marine and Earth Sciences and Technology

³Nelson Mandela Metropolitan University

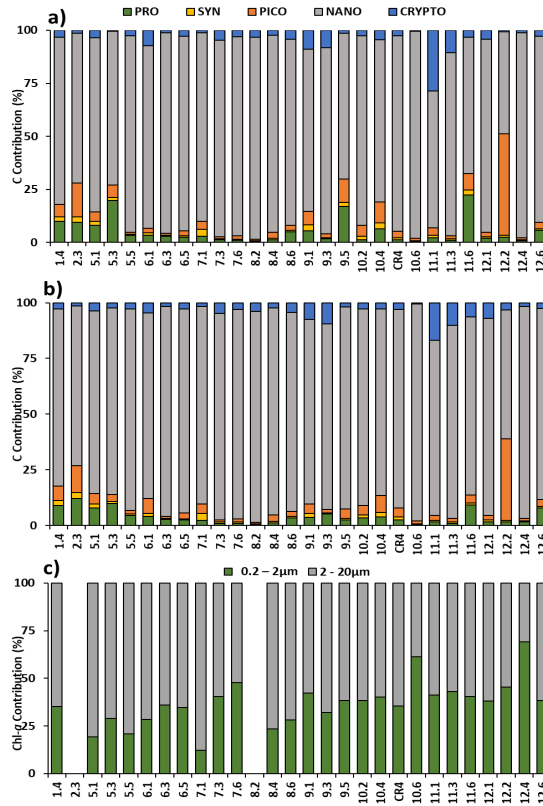
⁴Department of Biological Sciences and Marine Research Institute, University of Cape Town

April 05, 2024

Abstract

Autumn productivity is key to the large marine ecosystems of the Agulhas Bank, which support numerous economically important regional fisheries. Despite such importance, data is sparse on plankton composition in terms of primary or secondary producers, or on trophic transfer. While investigating autumn plankton composition we found that nanophytoplankton (2-20 μm) dominated carbon stocks, with lower contributions from picophytoplankton ($<2 \mu\text{m}$) and microphytoplankton ($>20 \mu\text{m}$). While picoplankton biomass exhibited a relationship with warm nutrient poor waters, nanoplankton showed no clear relationship to environmental parameters. The dominance of nanophytoplankton biomass on the Agulhas Bank highlights a critical role for micro-zooplankton grazing as a trophic transfer between these small plankton, meso-zooplankton and the higher trophic levels that make the bank so important for regional fisheries. Outside of localized coastal upwelling on the Agulhas Bank, this study highlights a significant role for nanoplankton and micro-zooplankton in supporting the bank's large marine ecosystems.

Figure 3. Phytoplankton group contributions (%) to total carbon biomass for surface waters (a) and integrated euphotic zone (b), and for integrated size fractionated Chl (c). PRO, SYN, PICO, NANO and CRYPTO. (c) size fractionated Chl (Poulton et al., 2022) for picoplankton (0.2-2 μm) and nanoplankton (2-20 μm) in the euphotic zone.



Hosted file

Mazwane Supplementary.docx available at <https://authorea.com/users/749716/articles/720956-nanoplankton-dominate-autumn-biomass-on-the-agulhas-bank>

Hosted file

Mazwane_Table 1.docx available at <https://authorea.com/users/749716/articles/720956-nanoplankton-dominate-autumn-biomass-on-the-agulhas-bank>

Figure 1. Phytoplankton biomass distribution on the Agulhas Bank in autumn. (a) Surface calibrated-fluorescence FChl (mg m^{-3}) superimposed on an 8-day composite (28/2/2019 – 06/3/2019) of satellite Chl (4 km Ocean Colour Climate Change Initiative (OCCI) data); euphotic zone integrated biomass (g C m^{-2}) of each group (b) PRO, (c) SYN, (d) PICO, (E) NANO, and (F) CRYPTO. Bathymetry marks the 200 m isobath.

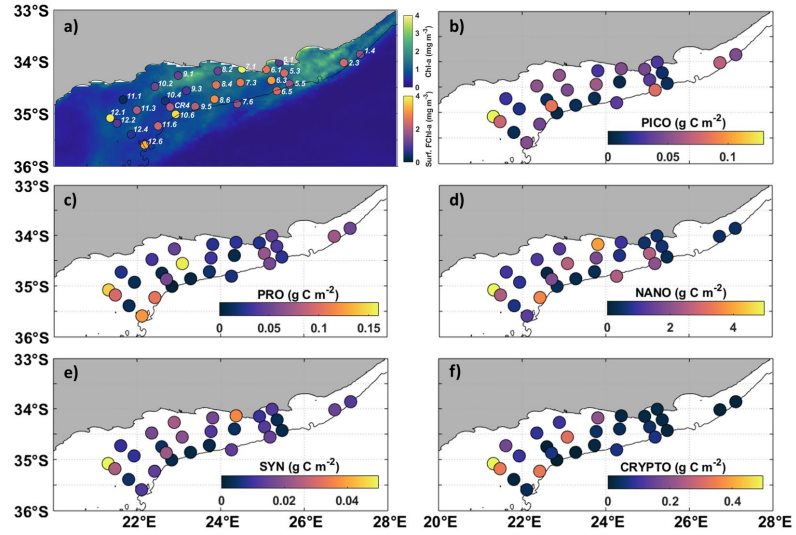
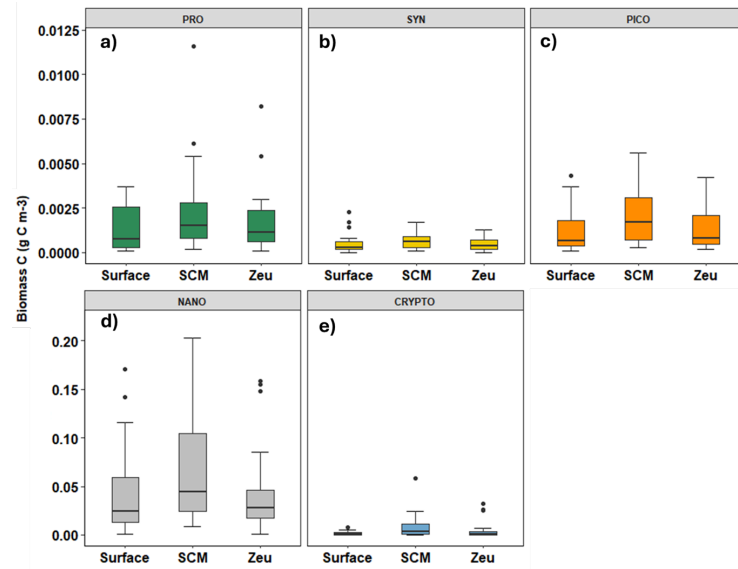


Figure 2. Boxplots of biomass (g C m^{-3}) in surface waters, the sub-surface chlorophyll maximum (SCM) and at the base of the euphotic depth (Z_{eu}) for each group (a) PRO, (b) SYN, (c) PICO, (d) NANO, and (e) CRYPTO. The boxplots indicate values of median (solid horizontal line), 25th and 75th percentiles (box ranges), confident intervals (whiskers), and outliers (black dots).



1 **Nanoplankton dominate autumn biomass on the Agulhas Bank**

2

3 **Sixolile L. Mazwane¹, Alex J. Poulton², Margaux Noyon¹, Emma Roche³, Mike J.**
4 **Roberts^{1,4}**

5

6 ¹Department of Oceanography and Institute for Coastal and Marine Research, Nelson Mandela
7 University, Port Elizabeth 6001, South Africa.

8 ²The Lyell Centre for Earth and Marine Science, Heriot-Watt University, Riccarton Campus,
9 Edinburgh, EH14 4AP, UK.

10 ³Department of Biological Sciences and Marine Research Institute, University of Cape Town, Cape
11 Town 7701, South Africa

12 ⁴School of Ocean and Earth Sciences, University of Southampton, Southampton, United Kingdom

13

14 Corresponding author: Sixolile Mazwane (Smazwane46@gmail.com)

15

16 **ORCID IDs**

17 Sixolile Mazwane (0000-0001-8707-3111)

18 Alex Poulton (0000-0002-5149-6961)

19 Margaux Noyon (0000-0002-0761-4174)

20 Emma Roche (0000-0001-9514-9788)

21 Mike Roberts (0000-0003-3231-180X)

22

23 **Key points:**

- 24 • Nanoplankton dominate carbon (>80% total) biomass in autumn on the Agulhas
25 Bank.
- 26 • Nanoplankton dominance highlights micro-zooplankton grazing for trophic transfer.
- 27 • Nanoplankton and micro-zooplankton key to productive Agulhas Bank ecosystems.

28

29 **Abstract**

30 Autumn productivity is key to the large marine ecosystems of the Agulhas Bank, which support
31 numerous economically important regional fisheries. Despite such importance, data is sparse
32 on plankton composition in terms of primary or secondary producers, or on trophic transfer.
33 While investigating autumn plankton composition we found that nanophytoplankton (2-20
34 μm) dominated carbon stocks, with lower contributions from picophytoplankton (<2
35 μm) and microphytoplankton (>20 μm). While picoplankton biomass exhibited a
36 relationship with warm nutrient poor waters, nanoplankton showed no clear relationship
37 to environmental parameters. The dominance of nanophytoplankton biomass on the Agulhas
38 Bank highlights a critical role for micro-zooplankton grazing as a trophic transfer between
39 these small plankton, meso-zooplankton and the higher trophic levels that make the bank so
40 important for regional fisheries. Outside of localized coastal upwelling on the Agulhas Bank,
41 this study highlights a significant role for nanoplankton and micro-zooplankton in supporting
42 the bank's large marine ecosystems.

43 **Plain Language Summary**

44 Phytoplankton support productive marine ecosystems through provision of primary
45 production and biomass, with their size-structure determining the efficiency of transfer of
46 energy through the ecosystem. Dominance of small phytoplankton (<20 μm) leads to longer
47 food chains and transfer of energy and biomass to higher trophic levels. Observations of
48 the Agulhas Bank plankton community in autumn, a period of important primary
49 productivity for the region, found a dominance of small nanoplankton (2-20 μm) in terms
50 of biomass. Nanoplankton dominance has important implications for how the Agulhas
51 Bank ecosystem function, highlighting a significant role for micro-zooplankton. The
52 Agulhas Bank is a data sparse environment currently no research on micro-zooplankton
53 has focused on the Agulhas Bank and this is an obvious important group to study further
54 to better understand how the marine ecosystem supports the key regional fisheries that rely
55 on this area.

56

57

58

59

60 1. Introduction

61

62 Phytoplankton support marine food webs and the carbon cycle, accounting for ~50% of global
63 net primary production (Field et al., 1998). Plankton size structure constrains ecosystem
64 productivity (Marañón, 2015), determining the proportion of production passed to higher
65 trophic levels, recycled or exported to the deep sea (Acevedo-Trejos et al., 2015).
66 Phytoplankton may be split into different size categories (Sieburth, 1979): picoplankton (cell
67 diameters 0.2-2 μm), nanoplankton (2-20 μm) and microplankton ($>20 \mu\text{m}$). The small cell
68 diameters of pico- and nano-plankton are not grazed by meso-zooplankton ($>200 \mu\text{m}$) (Huggett
69 et al., 2023, Mitra et al., 2023), and instead are predated by micro-zooplankton (20-200 μm)
70 who then may be grazed by larger zooplankton.

71 Picoplankton are made up of the cyanobacteria *Prochlorococcus* (PRO) and *Synechococcus*
72 (SYN) (Waterbury et al., 1979; Chisholm et al., 1988; Rajaneesh et al., 2017), and a diverse set
73 of pico-eukaryotes (PICO) (Worden, 2006). SYN and PICO favor light and nutrient rich waters
74 (Moore et al., 2003; Rajaneesh et al., 2015). Nanoplankton (NANO, 2-20 μm) include a diverse
75 number of taxa, including Haptophytes, Pelagophytes, and Cryptophytes (CRYPTO) (Flander-
76 Putrle et al., 2021), with haptophytes often dominating (Liu et al., 2009). Larger microplankton
77 ($>20 \mu\text{m}$) are most frequently associated with diatoms and dinoflagellates (Rajaneesh et al.,
78 2017; Lamont et al., 2018).

79 PRO and SYN have overlapping ecological niches of warm low-nutrient waters and
80 may contribute up to 80% of phytoplankton biomass and productivity (Scanlan et al., 2009;
81 Wang et al., 2022), despite their relatively small size (0.5-0.7 μm and 0.7-1.2 μm ,
82 respectively) and cell carbon content (Tarran et al., 2006). PICO are typically less abundant
83 than PRO or SYN by at least an order of magnitude (Flombaum et al., 2020), though
84 they contribute more to biomass due to their larger cell size (0.2-3 μm) and carbon content
85 (Moran, 2015).

86 Shelf seas make a disproportional contribution to primary production compared to their areal
87 extent (Field et al., 1998), supporting ~ 90% of economically important fisheries (Pauly et al.,
88 2002). Shelf seas are often regarded as microplankton dominated, though little is known of the
89 smaller plankton in these systems (van Dongen-Vogels et al., 2011, 2012; Daneri et al., 2012).

90

91 The Agulhas Bank (AB) is a moderately productive shelf (Mazwane et al., 2022) that supports
92 complex trophic structures and numerous commercially harvested marine resources (Hutchings
93 et al., 2009; Lamont et al., 2018). Analysis of satellite and pigment data from the AB has
94 highlighted microplankton dominance in inner shelf waters, with nanoplankton in the adjacent
95 ocean (Barlow et al., 2010; Lamont et al., 2018; Sonnekus, 2022), though such studies have
96 focused on the eastern AB rather than the wider bank.

97 To explore the gap in knowledge of the AB plankton in terms of pico- and nano-plankton, we
98 undertook flow cytometry (Marie et al., 1997; van Dongen-Vogels et al., 2011) of the small
99 phytoplankton (<20 μm) during an autumn (2019) cruise (Figure 1a). Our objectives were to
100 determine the (1) pico- and nano-plankton composition and distribution, (2) contribution of
101 these groupings to carbon biomass, and (3) explore whether variability in composition and
102 biomass were related to prevailing hydrographic gradients.

103 **2. Material and Methods**

104 **2.1. Sampling**

105 Sampling occurred on the AB onboard the *RV Ellen Khuzwayo* (cruise EK188, Noyon
106 (2019), 21 March to 2 April 2019; $n = 28$) (Figure 1a). A Seabird 911+ V2 CTD system
107 with rosette sampler was deployed, with water samples collected using 8 L Niskin bottles
108 (OTE: Ocean Test Equipment), and sampling depths determined from temperature and
109 fluorescence (WET Labs) profiles. Processing and calibration of CTD data followed
110 standard procedures (see Noyon, 2019).

111 A CTD-mounted quantum PAR sensor (LiCor Inc., USA) determined the underwater light
112 field and vertical attenuation coefficient of PAR (K_d , m^{-1}), with the depth of the euphotic zone
113 as the depth that 1% surface irradiance penetrates (Poulton et al. 2022). Sea-surface
114 Temperature (SST) was measured *in-situ* using a CTD-mounted temperature sensor. The
115 surface mixed layer (SML) was determined as the depth of the maximum buoyancy
116 frequency (Carvalho et al., 2017), with the maximum (N^2 max.) value used as a
117 stratification index (Poulton et al., 2022). Average SML irradiance (\bar{E}_{SML}) was determined
118 using a combination of K_d and SML (Poulton et al., 2011).

119

120

121 2.2. Flow Cytometry

122

123 Flow cytometry samples were collected from 4-5 depths, including sub-surface waters (~3
124 m), the beginning, maximum and lower limit of the fluorescence maximum, and below
125 the strongest temperature gradient (thermocline). Seawater samples were pre-filtered through
126 200 μm mesh to remove zooplankton, and 2 mL triplicate aliquots were fixed in
127 0.25% glutaraldehyde (v/v, final concentration), flash frozen and stored (-80°C) prior to
128 analysis.

129 Cell abundances (after Marie et al., 1997; van Dongen-Vogels et al., 2011) were determined
130 on a LSRII (Becton Dickinson) flow cytometer with a 488-nm excitation laser and standard
131 filter set (Campbell, 2001). FlowJo® software calculated PRO and SYN cell abundances.
132 PICO, NANO and CRYPTO were measured through their respective signals emitted in
133 orange (PE: 585/42 band pass) versus red (PC: 661/16 band pass) wavelengths. SYN
134 abundance was distinguished from PICO and PRO through higher (per cell)
135 phycoerythrin signals. The samples were thawed at room temperature and transferred to
136 glass tubes and analyzed. Data were acquired at a medium flow rate with a threshold of
137 ~10,000 events per run and the LSRII was calibrated daily using 3.0 μm Rainbow beads
138 (Spherotech).

139 Cell abundances (cells mL^{-1}) were calculated from the mean of the triplicate samples, with
140 relative standard deviations between triplicates ranging from 1-54% (average: 20%). Cell
141 abundances were converted to cell biomass using literature values (Børsheim and Bratbak,
142 1987; Tarran et al., 2006): 2.7 fmol C cell^{-1} , Prochlorococcus (PRO); 8.58 fmol C cell^{-1} ,
143 Synechococcus (SYN); 36.67 fmol C cell^{-1} for pico-eukaryotes (PICO); 0.26 pmol C cell^{-1} for
144 nanoeukaryotes (NANO); 0.26 pmol C cell^{-1} , for cryptophytes (CRYPTO).

145 For this study, the biomass integrations were calculated for the euphotic depth and MLD (see
146 Table S1). The conversion values were chosen as values previously used for shelf waters
147 rather than the open ocean. For NANO and CRYPTO, we used values from Børsheim and
148 Bratbak (1987). Using Tarran et al. (2006) values would increase the NANO and CRYPTO
149 biomass by 6.8% without changing the biomass patterns.

150

151 **2.3. Size-fractionated Chlorophyll-*a* and Nutrients**

152 Size-fractionated chlorophyll-*a* (Chl) concentrations (mg m^{-3}) were measured on 0.2 L water
153 samples sequentially filtered through 20 μm , 2 μm and 0.2 μm 47-mm NucleoporeTM filters
154 and extracted in 6 mL 90% acetone (Sigma-Aldrich, UK) at 4°C for 18-24 hr (Poulton et al.,
155 2022). Chl fluorescence was measured on a Turner Designs TrilogyTM fluorometer using a
156 non- acidification unit calibrated with solid and pure Chl standards (Sigma-Aldrich, UK).

157 Water samples for macronutrient concentrations were collected into acid-cleaned 50 mL
158 HDPE bottles, which were frozen (-20°C) onboard and kept frozen until analysis (see Poulton
159 et al., 2022). Concentrations ($\mu\text{mol L}^{-1}$) of nitrate + nitrite (NO_3), phosphate (PO_4) and silicic
160 acid ($\text{Si}(\text{OH})_4$) were measured with a SEAL QuAAtro39 auto-analyzer following standard
161 protocols (Becker et al., 2020). Certified reference materials were used daily (KANSO,
162 Japan) and analytical procedures followed International GO-SHIP recommendations (Becker
163 et al., 2020). The typical uncertainty of the analytical results were between 0.5% and 1%, and
164 the limits for detection for NO_3 and PO_4 were $0.02 \mu\text{mol L}^{-1}$, while $\text{Si}(\text{OH})_4$ was always
165 higher than the detection limit ($0.05 \mu\text{mol Si L}^{-1}$). Deficiencies of NO_3 relative to PO_4 and
166 $\text{Si}(\text{OH})_4$ were described relative to the Redfield (1958) ratio, with N^* ($= \text{NO}_3 - (16 \times \text{PO}_4)$;
167 Moore et al., 2009), and relative to the 1:1 ratio of $\text{Si}(\text{OH})_4$ to NO_3 uptake in diatoms
168 (Brzezinski, 1985) through Si^* ($= \text{Si}(\text{OH})_4 - \text{NO}_3$; Bibby and Moore, 2011).

169 **3. Results**

170 **3.1. Agulhas Bank Hydrography**

171 A comprehensive overview of the hydrography of the AB during autumn (2019) is provided
172 by Poulton et al. (2022), with the data included in Supplementary Table S1. SST ranged from
173 $17\text{-}22^{\circ}\text{C}$ (average (\pm standard deviation): $20 (\pm 1)^{\circ}\text{C}$) across the AB, with offshore stations
174 generally showing higher SST (Table S2). SML in autumn showed an east (<10 m) to west
175 (>20 m) deepening (Table S2), with the deepest SML at 27 m (average: $15 (\pm 5)$ m). SML
176 deepening was related to warming of the SML, linked to the westward SST increase (Poulton
177 et al., 2022). No clear or consistent inshore-offshore trends in the SML depth or SST were
178 observed.

179 Euphotic zone depths ranged from 23-53 m (Table S2), with an average of 33 m (± 7 m) and
180 no clear east to west or inshore-offshore trend was observed. ESML indicated that
181 phytoplankton in the SML received irradiances ranging from 26-63% (average: $44 (\pm 10)$ %)

182 of the incidental irradiance (Table S2). An east to west trend was observed, with the
183 irradiance decreasing towards the west as the SML deepened (Table S1, Poulton et al., 2022).

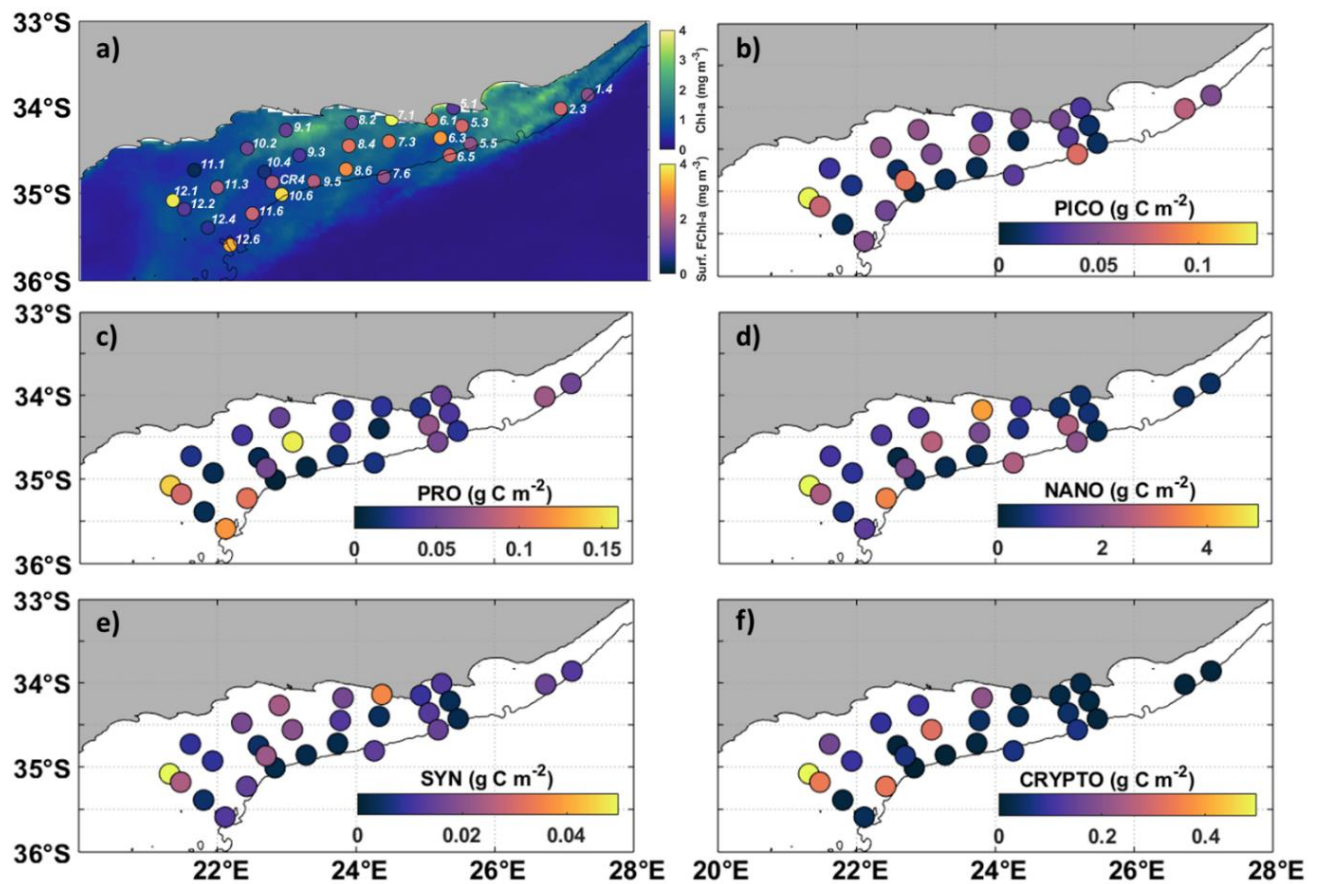
184 The maximum value of the buoyancy frequency (N^2 max.), an indicator of water column
185 stratification, showed an east to west strengthening (Table S2), from values $<4 \times 10^3 \text{ s}^{-2}$ in the
186 east to $\sim 5 \times 10^3 \text{ s}^{-2}$ in the west. Increasing stratification from east to west likely relates to
187 warming of SST, and interactions with the Agulhas Current (Poulton et al., 2022).

188 SML NO_3 ranged from 0.1-6.2 $\mu\text{mol N L}^{-1}$ (average: $1.1 (\pm 1.4) \mu\text{mol N L}^{-1}$), with similar
189 concentrations in the east and west (Table S2). Relative to PO_4 , as indicated by N^* values,
190 NO_3 was always deficient (always negative) relative to Redfield (1958) (Table S2, Poulton et
191 al., 2022). Strong negative values (-6 to -2.5) were related to the subtropical source waters for
192 the AB (Poulton et al., 2022). SML $\text{Si}(\text{OH})_4$ ranged from 0.6-5.1 $\mu\text{mol Si L}^{-1}$ (average: $2.9 (\pm$
193 $1.1) \mu\text{mol Si L}^{-1}$) (Table S2), higher than those found in the subtropical source water and
194 highlighting the role of coastal upwelling in (re)supplying and retaining Si on the AB
195 (Poulton et al., 2022). SML Si^* values were mostly positive on the AB indicating residual
196 silicic acid relative to NO_3 in autumn (Table S2).

197 **3.2. Spatial Distribution of Phytoplankton Biomass**

198 Satellite Chl concentrations ranged from <0.1 - 4.0 mg m^{-3} during autumn, with higher
199 concentrations from east to west (Figure 1a). Surface in-situ Chl ranged from 0.3 - 4.7 mg m^{-3}
200 (average: $2.1 (\pm 1.1) \text{ mg m}^{-3}$) (Figure 1a). Around 46% of sampling stations had Chl $>2 \text{ mg}$
201 m^{-3} and no consistent spatial distribution was observed.

202 In terms of euphotic zone integrated biomass, PRO biomass ranged from 0.002 - 0.16 g C m^{-2}
203 (average: $0.05 (\pm 0.04) \text{ g C m}^{-2}$) (Figure 1b). SYN biomass ranged from 0.002 - 0.05 g C m^{-2}
204 ($0.01 (\pm 0.01)$) and was relatively high ($>0.02 \text{ g C m}^{-2}$) at some of the inshore stations (e.g.,
205 transects 7, 9 and 12), while offshore stations exhibited lower ($<0.01 \text{ g C m}^{-2}$) biomass
206 (Figure 1c). Of all the groups, SYN biomass was the lowest. PICO biomass ranged from
207 0.006 - 0.13 g C m^{-2} (average: $0.04 (\pm 0.03) \text{ g C m}^{-2}$) (Figure 1d). NANO dominated biomass,
208 with estimates ranging from 0.19 - 4.99 g C m^{-2} (average: $1.4 (\pm 1.2) \text{ g C m}^{-2}$) (Figure 1e).
209 NANO biomass was much higher ($>0.3 \text{ g C m}^{-2}$) than the other groups at $\sim 100\%$ of stations.
210 CRYPTO biomass ranged from 0.002 to 1.09 g C m^{-2} (average: $0.12 (\pm 0.22) \text{ g C m}^{-2}$) (Figure
211 1f). No clear spatial patterns were observed for PRO, SYN, PICO, or NANO (Figures 1b-e),
212 though there was a noticeable increase in CRYPTO biomass from east to west (Figure 1f).



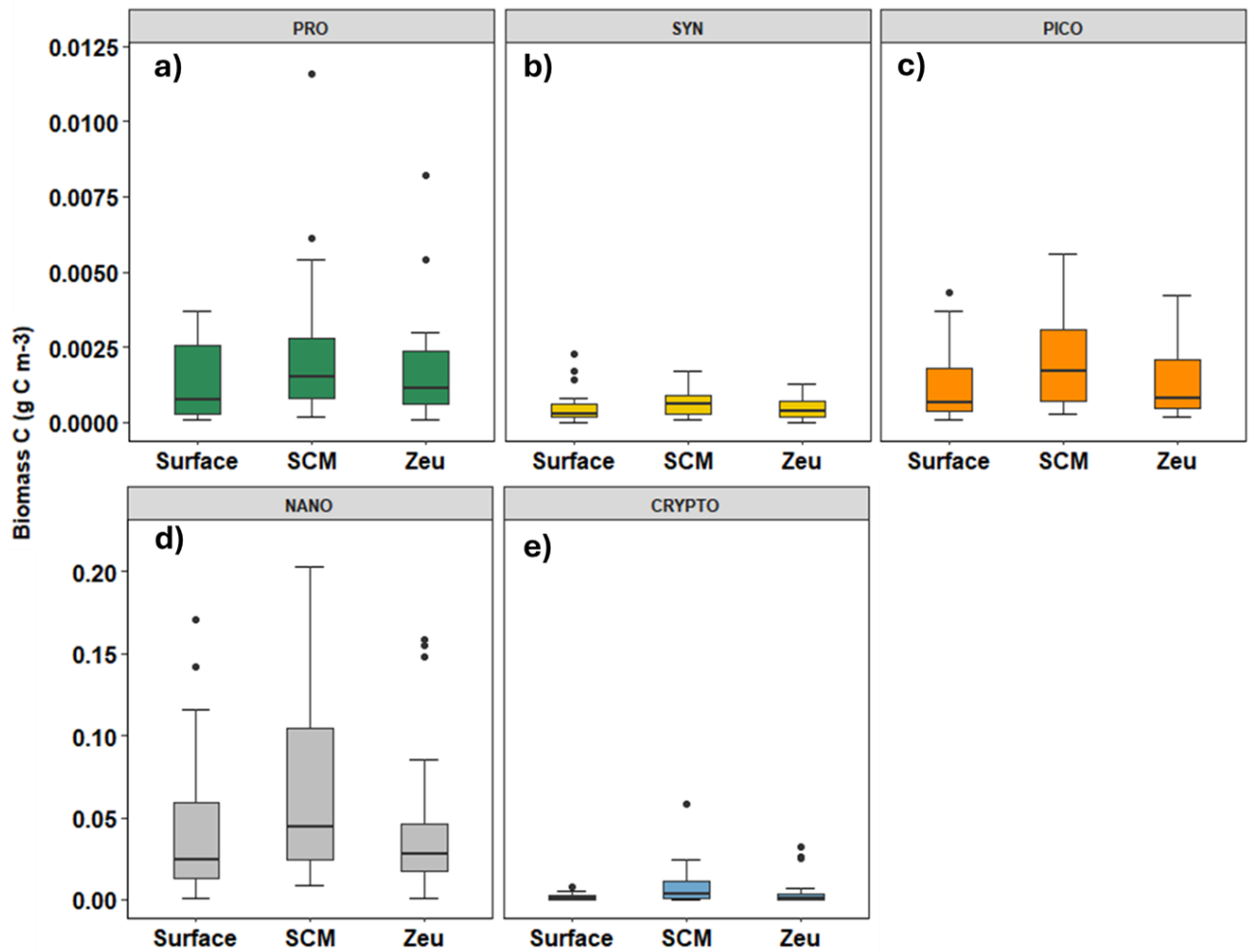
213

214 **Figure 1.** Phytoplankton biomass distribution on the Agulhas Bank in autumn. (a) Surface
 215 calibrated-fluorescence FChl (mg m^{-3}) superimposed on an 8-day composite (28/2/2019 –
 216 06/3/2019) of satellite Chl (4 km Ocean Colour Climate Change Initiative (OCCI) data);
 217 euphotic zone integrated biomass (g C m^{-2}) of each group (b) PRO, (c) SYN, (d) PICO, (E)
 218 NANO, and (F) CRYPTO. Bathymetry marks the 200 m isobath.

219 3.3. Vertical Distribution of Phytoplankton Biomass

220 A sub-surface Chl maximum (SCM) occurred at ~50% of the stations sampled on the AB
 221 (Poulton et al., 2022), ranging in depth from 9 to 41 m and exhibiting no clear spatial pattern
 222 between stations. Generally, the vertical distribution of the different groups in terms of biomass
 223 was variable amongst the sampled stations. The depth of maximum biomass varied throughout
 224 the sampled stations and between the different groups. To examine the vertical distribution of
 225 small phytoplankton biomass, box-and-whisker plots of group biomass concentrations for
 226 surface waters, the SCM and at the base of the euphotic zone (Z_{eu}) are presented in Figure 2.
 227 None of the five groups examined (PRO, SYN, PICO, NANO, CRYPTO) showed any general
 228 depth preferences (Kruskal-Wallis t-tests, $p > 0.05$ for all groups and depth), though the
 229 median biomass for all groups was slightly higher in the SCM than surface or deeper waters

230 (Figures 2a-e). Overall, NANO exhibited higher biomass ($>0.05 \text{ g C m}^{-3}$; Figure 2d) than
 231 all the other groups for the depths examined (Figures 2a-e).



232

233 **Figure 2.** Boxplots of biomass (g C m^{-3}) in surface waters, the sub-surface chlorophyll
 234 maximum (SCM) and at the base of the euphotic depth (Zeu) for each group (a) PRO, (b)
 235 SYN, (c) PICO, (d) NANO, and (e) CRYPTO. The boxplots indicate values of median
 236 (solid horizontal line), 25th and 75th percentiles (box ranges), confident intervals
 237 (whiskers), and outliers (black dots).

238

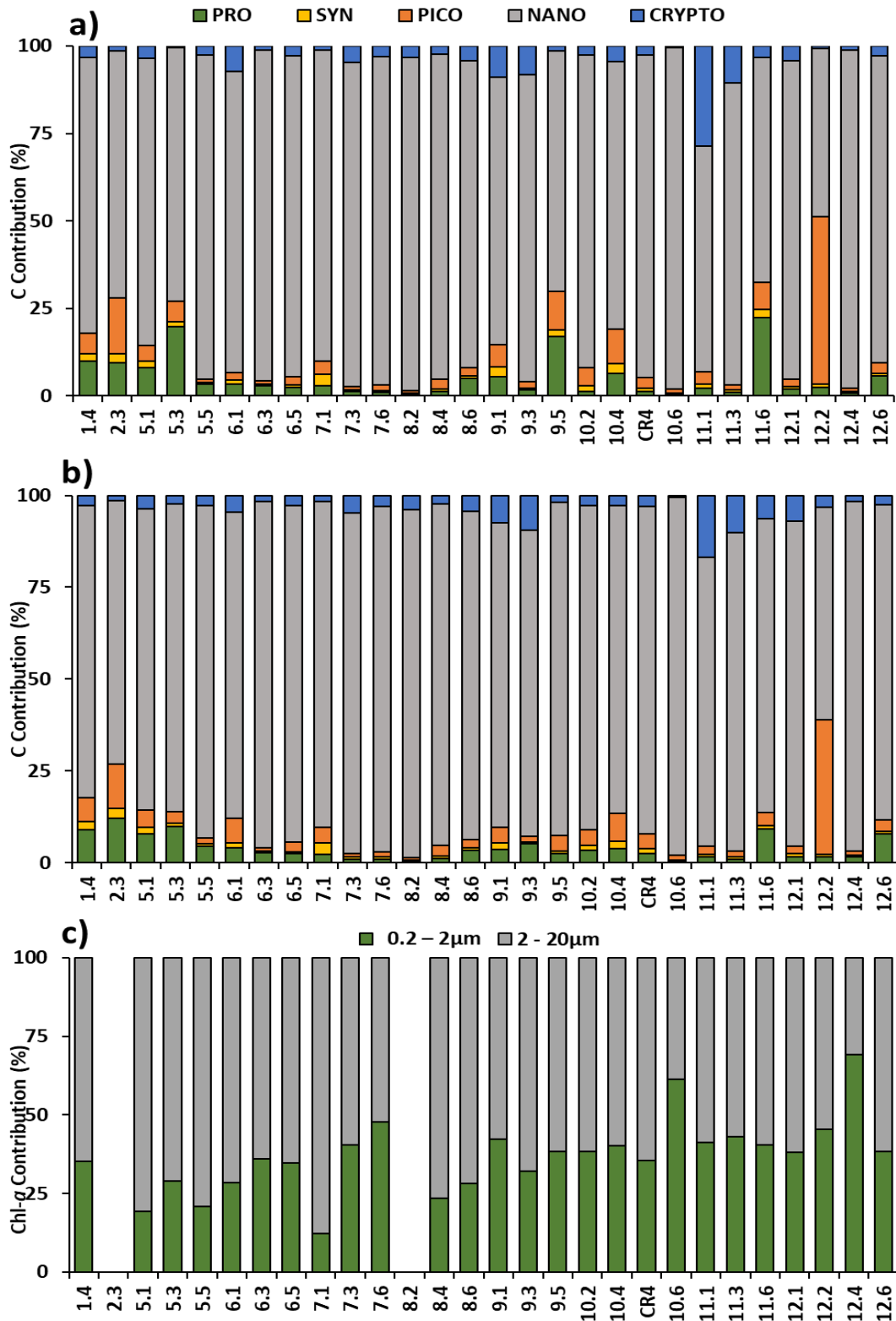
239 3.4. Size-structure of the Phytoplankton Community

240 In surface waters, NANO dominated (average: $85 (\pm 9.9) \%$) community biomass (Figure 3a),
 241 with lower and more similar average contributions from PRO ($5.1 (\pm 5.8) \%$), CRYPTO (4.4
 242 $(\pm 5.4) \%$) and PICO ($4.0 (\pm 3.6) \%$), and much lower contributions from SYN ($1.3 (\pm 0.9)$
 243 $\%$). NANO contributions to surface phytoplankton biomass were always $>70\%$, while PRO

244 contributions were always <15% and only at 6 stations were the contributions >5% (Figure
245 3a). SYN contributions to surface phytoplankton biomass were always <3%, while PICO and
246 CRYPTO were always less than 20% and 15%, respectively.

247 For euphotic zone integrated biomass (Figure 3b), NANO were again dominant ($87 (\pm 5.7)$
248 %), with lower and more similar contributions from CRYPTO ($4.9 (\pm 4.1)$ %), PRO ($3.6 (\pm$
249 $2.8)$ %) and PICO ($3.3 (\pm 2.4)$ %), and SYN contributions $\sim 1\%$ ($1.1 (\pm 0.7)$ %). PRO biomass
250 contribution decreased on average from east to west (5.0 to 2.8%) while CRYPTO
251 contributions increased east to west (2.8 to 6.2%), whereas no clear trend was evident for the
252 other groups. Low (<2%) contributions for SYN were a consistent feature in both surface
253 waters (Figure 3a) and integrated biomass over the euphotic zone on the AB in autumn
254 (Figure 3b).

255 Whether in carbon (Figures 3a & b) or Chl-a biomass (Figure 3c; Poulton et al., 2022), the
256 nanoplankton (2-20 μm) were the dominant size class on the AB in autumn. On average,
257 nanoplankton Chl (NANO+CRYPTO) represented $63.1 (\pm 11.9)$ % of total Chl-a, while
258 picoplankton Chl (PRO+SYN+PICO) represented $36.9 (\pm 11.9)$ % (Figure 3c). Picoplankton
259 contributions to total Chl-a increased east to west (30.4 to 41.0%), while nanoplankton Chl
260 decreased east to west (69.6 to 59.0%). Measurements of microplankton Chl (>20 μm ;
261 Poulton et al., 2022) showed low contributions (<30%) across most of the AB, with few
262 stations characterised by microplankton dominance (not shown).



263

264 **Figure 3.** Phytoplankton group contributions (%) to total carbon biomass for surface waters
 265 (a) and integrated euphotic zone (b), and for integrated size fractionated Chl (c). PRO, SYN,
 266 PICO, NANO and CRYPTO. (c) size fractionated Chl (Poulton et al., 2022) for picoplankton
 267 (0.2-2 μm) and nanoplankton (2-20 μm) in the euphotic zone.

268 **3.5. Phytoplankton Biomass and Agulhas Bank Hydrography**

269 To explore the relationship between environmental conditions and phytoplankton
 270 composition, variability in hydrography (SST, \bar{E}_{SML} , N^2 max., and SML average nutrient
 271 concentrations [NO_3 , $Si(OH)_4$]) was assessed with a Principal Component Analysis (PCA) (R
 272 vegan package). PC1 explained 44% of the variance between stations, while PC2 explained
 273 27% and three next PCs explained less than 15% each. PC1 describes an inverse relationship
 274 between SST and nutrient (NO_3 , $Si(OH)_4$) concentrations (Table 1); warmer waters were
 275 more nutrient poor on the AB. PC2 describes an inverse relationship between stratification
 276 (N^2 max.) and \bar{E}_{SML} (Table 1); with stronger stratification leading to shallower SML and
 277 higher average irradiances.

278 Though PC1 and PC2 reflected the spatial variability in hydrographic conditions across the
 279 AB (see also Poulton et al., 2022), Pearson correlation showed that there was limited co-
 280 variability with phytoplankton biomass or community composition (Table 1). Only the
 281 absolute biomass of PICO and SYN showed (negative) statistically significant ($p < 0.05$)
 282 correlations with PC1; no statistically significant correlations were observed with the biomass
 283 of the other groups present on the AB (Table 1). This highlights higher biomass of PICO and
 284 SYN warmer, more nutrient poor waters on the AB. No correlations were observed between
 285 either PCs and the percentage contribution of the different groups to total biomass (Table 1).

286 **Table 1.** Results of Principal Component Analysis (PCA), including eigenvalues and Pearson
 287 correlation coefficients for the relationships between PC scores, hydrographic variables, and
 288 absolute and relative phytoplankton group biomass (n = 28). * $p < 0.05$; ** $p < 0.01$; *** $p <$
 289 0.005.

<i>Hydrography</i>	SST	\bar{E}_{SML}	N^2 max.	SML NO_3	SML $Si(OH)_4$
PC-1	-1.4 (-0.92***)	0.44 (0.29)	-0.39 (-0.26)	1.30 (0.85***)	1.06 (0.70***)
PC-2	-0.28 (-0.19)	-1.04 (-0.68***)	1.14 (0.75***)	-0.26 (-0.17)	0.79 (0.52**)
	PRO	SYN	PICO	NANO	CRYPTO
<i>Absolute Biomass</i>					
PC-1	-0.36	-0.41*	-0.45*	-0.27	-0.28
PC-2	-0.09	0.2	-0.004	-0.06	0.06
<i>Relative Biomass</i>					
PC-1	-0.02	-0.10	-0.1	0.29	-0.32
PC-2	-0.26	0.17	-0.07	0.03	0.16

291 4. Discussion

292 The average integrated biomass for the pico- and nanoplankton on the AB in autumn was 1.6
293 g C m^{-2} (range: 0.2 to 6.4 g C m^{-2}) which agrees well with a value of 1.9 g C m^{-2} for the global
294 ocean (Buitenhuis et al., 2012) and $\sim 2.2 \text{ g C m}^{-2}$ for similar regional shelf sea studies (e.g.,
295 Agusti et al., 2019; Wei et al., 2020; Chen et al., 2021). Overall, NANO showed the highest
296 contribution (average: 87%; range: 73 to 96%) to the total carbon biomass in surface, SCM
297 and integrated over the water column, with all other groups contributing less than 5%.
298 Dominance of phytoplankton biomass by nanoplankton agrees well with the size fractionated
299 pigment data from Poulton et al. (2022), highlighting higher contributions to total Chl of
300 nanoplankton than either pico- or microplankton.

301 On the east coast of South Africa, Barlow et al. (2002, 2020) reported elevated biomass and
302 a co-dominance between diatoms and haptophytes on the far eastern stations between 26.5
303 and 27.5°E due to the upwelling of nutrient rich waters. This is indicative of the
304 nanoplankton dominance in the region upstream (east) of our sampling area. Lamont et al.
305 (2018) also highlighted nanoplankton as important to the AB despite showing a lower
306 contribution than microplankton. The nano-sized group has been observed to be more
307 prominent in warmer shelf waters, where they are able to take advantage of high nutrient
308 concentrations (Barlow et al., 2001, 2017).

309 Despite the highly stratified nature of the AB (Carter et al., 1987; Largier and Swart, 1987),
310 the distribution of pico- and nanoplankton biomass for the different groups showed no
311 strong vertical patterns (Figure 2). Though biomass of all groups was slightly higher in the
312 SCM, these differences were not statistically significant and the SCM did not represent a
313 strong biomass maximum as found in other shelf sea systems (e.g., Mena et al., 2019;
314 Barnett et al., 2019). During autumn on the AB, light availability in the SCM decreased
315 from east to west (Poulton et al., 2022), this is likely linked to peak biomass observed on
316 some stations on the west, and thus may have prevented strong biomass maxima forming at
317 depth. Previous studies on the central AB have observed SCM with considerable Chl
318 concentrations ($>10 \text{ mg m}^{-3}$) and phytoplankton biomass (Carter et al., 1987), though such
319 high Chl SCM were not observed during autumn in 2019.

320 While the AB had identifiable gradients in hydrographic conditions, as recognised in the PCA
321 (Table 1) and other related studies (Poulton et al., 2022; Noyon et al., 2022), there were few

322 clear relationships between phytoplankton group biomass or community composition. Only
323 PRO and SYN biomass correlated with PC1, indicating that these groups had higher biomass
324 in warmer, more nutrient impoverished waters, potentially linked to the offshore Agulhas
325 Current (Probyn et al., 1994; Jackson et al., 2012; Malan et al., 2018). This lack of linkage
326 between phytoplankton biomass and composition potentially relates to non-limiting nutrient
327 and light conditions (Poulton et al., 2022) across the section of the bank sampled in autumn
328 2019 (i.e., not near coast or off shelf waters).

329 Alternatively, nanoplankton dominance on the AB in autumn may be linked to the importance
330 of grazing in controlling community composition. Indeed, a strong link between NPP and
331 secondary production was observed in autumn 2019 (Noyon et al., 2022; Poulton et al.,
332 2022), and an importance of microzooplankton as active grazers and agents of trophic transfer
333 on the bank has been highlighted before (Huggett et al., 2023). Globally, ~64% of
334 phytoplankton daily primary production is grazed by micro-zooplankton, with the smaller
335 pico- and nanoplankton readily grazed by planktonic ciliates, heterotrophic flagellates, and
336 small zooplankton (Calbet and Landry, 2004; Mayers et al., 2019).

337 With the warming of the ocean, it is expected that the phytoplankton will shift from large-
338 species dominance to smaller nano-sized phytoplankton (Bopp et al., 2005; Lomas et al.,
339 2012; Dutkiewicz et al., 2013; Henson et al., 2021). This will in turn have a large impact on
340 the grazers, suggesting a decrease in food quality and a shift in the size structure of
341 zooplankton from large to smaller groups (Safi et al., 2023). Our study further highlights the
342 importance of microzooplankton on the AB in autumn, warranting further attention on these
343 organisms in supporting the ecosystems of the AB.

344 A shift in the global trends of phytoplankton size structure from large to smaller sized
345 phytoplankton has previously been observed and is projected in the future (Bopp et al., 2005;
346 Lomas et al., 2012; Dutkiewicz et al., 2013; Henson et al., 2021). This is mainly attributed to
347 the warming of the oceans and a depletion of nutrient supplies, giving advantage to the nano-
348 and picoplankton communities to flourish. The dominance of nanoplankton biomass on the
349 AB shelf ecosystem is comparable to other shelf regions. A similar shift in the community
350 from the larger phytoplankton to the smaller phytoplankton was also indicated by Huggett et
351 al. (2023). On the AB, where there has been a scarcity of in-situ sampling of the plankton
352 community, shifts in size structure may have severe implications for the ecosystems
353 supported by AB productivity and there is an urgent need for further studies.

354 **Author contributions**

355 **Conceptualization:** Sixolile L. Mazwane, Alex J. Poulton, Margaux Noyon. **Formal**
356 **analysis:** Sixolile L. Mazwane, Alex J. Poulton, Margaux Noyon, Emma Rocke.
357 **Investigation:** Sixolile L. Mazwane, Alex J. Poulton. **Methodology:** Sixolile L. Mazwane,
358 Alex J. Poulton, Margaux Noyon, Emma Rocke. **Writing – original draft:** Sixolile L.
359 Mazwane, Alex J. Poulton, Margaux Noyon. **Writing – review & editing:** Sixolile L.
360 Mazwane, Alex J. Poulton, Margaux Noyon, Emma Rocke. **Project administration and**
361 **Funding Acquisition:** Mike J. Roberts.

362 **Conflict of interest**

363 The authors declare no conflicts of interest relevant to this study.

364 **Data Availability Statement**

365 Chlorophyll, CTD and nutrient data from EK188 is available through the British
366 Oceanographic Data Centre (BODC) at doi:10.5285/d5cea266-fbec-7ef0-e053-6c86abc0722c.
367 Flow cytometry count data has been submitted to Zenodo and can be accessed at
368 <https://doi.org/10.5281/zenodo.10674482>.

369 **Acknowledgements**

370 We thank the captain and crew of the R/V *Ellen Khuzwayo*, together with the Department of
371 Forestry, Fisheries, and the Environment (DFFE). This study was produced with the
372 financial support of the Global Challenges Research Fund (GCRF), UK, in the framework of
373 the SOLSTICE-WIO project, under NERC grant NE/P021050/1. This work was also part of
374 the UK-SA bilateral chair Ocean Science and marine food security funded by the NRF/DST
375 Grant (98399) and the British Council grant SARCI150326116102. We thank the Health
376 Sciences department at the University of Cape Town (UCT) for the use of their Flow
377 Cytometer. We would like to thank the ESA Ocean Colour CCI project for processing and
378 providing the *Chl-a* dataset online at <http://www.esa-oceancolour-cci.org/>.

379 **References**

380 Acevedo-Trejos, E., Brandt, G., Bruggeman, J., & Merico, A. (2015). Mechanisms shaping
381 size structure and functional diversity of phytoplankton communities in the ocean.
382 Scientific Reports, 5, 17–20. <https://doi.org/10.1038/srep08918>

- 383 Agusti, S., Lubián, L.M., Moreno-Ostos, E., Estrada, M., & Duarte, C.M., 2019. Projected
384 Changes in Photosynthetic Picoplankton in a Warmer Subtropical Ocean. *Front. Mar.*
385 *Sci.* 5:506. doi: 10.3389/fmars.2018.00506
- 386 Barlow, R. G., Lamont, T., Kyewalyanga, M., Sessions, H., Morris, T., Carter, R. A., et al.
387 (2001). Chapter 6 : Latitudinal Changes in the Shape, Formation and Ecology of the
388 Chlorophyll a Maximum in the Subtropical and. *South African Journal of Marine*
389 *Science*, 54(1), 525–536. <https://doi.org/10.1016/j.rse.2017.09.038>
- 390 Barlow, R. G., Aiken, J., Holligan, P. M *Oceanographic Research Papers*, 49(4), 637–660.
391 [https://doi.org/10.1016/S0967-0637\(01\)00081-4](https://doi.org/10.1016/S0967-0637(01)00081-4)
- 392 Barlow, R., Lamont, T., Kyewalyanga, M., Sessions, H.,., Cummings, D. G., Maritorena, S.,
393 & Hooker, S. (2002). Phytoplankton pigment and absorption characteristics along
394 meridional transects in the Atlantic Ocean. *Deep-Sea Research Part I: & Morris, T.*
395 (2010). *Phytoplankton production and physiological adaptation* 30(13), 1472–
396 1486. <https://doi.org/10.1016/j.csr.2010.05.007>
- 397 Barlow, R., Lamont, T., Gibberd, M. J., Airs, R., Jacobs, L., & Britz, K. (2017).
398 Phytoplankton communities and acclimation in a cyclonic eddy in the southwest
399 Indian Ocean. *Deep-Sea Research Part I: Oceanographic Research*
400 *Papers*, 124, 18–30. <https://doi.org/10.1016/j.dsr.2017.03.013>
- 401 Barlow, R., Lamont, T., Gibberd, M. J., Russo, C., Airs, R., Tutt, G., et al. (2020).
402 Phytoplankton adaptation and absorption properties in an Agulhas Current ecosystem.
403 *Deep-Sea Research Part I: Oceanographic Research Papers*, 157(December 2019),
404 103209. <https://doi.org/10.1016/j.dsr.2019.103209>
- 405 Barnett, M.L., Kemp, A.E.S., Hickman, A.E. & Purdie, D.A. (2019). Shelf Sea subsurface
406 chlorophyll maximum thin layers have a distinct phytoplankton community structure.
407 *Continental Shelf Research*, Volume 174, 2019, 140-157,
408 <https://doi.org/10.1016/j.csr.2018.12.007>.
- 409 Becker, S., Aoyama, M., Woodward, E.M.S., Bakker, K., Coverly, S., Mahaffey, C., &
410 Tanhua, T.(2020). GO-SHIP repeat hydrography nutrient manual: the precise and
411 accurate determination of dissolved inorganic nutrients in seawater, using continuous
412 flow analysis methods. *Front. Mar. Sci.* 7, 581790.
413 <https://doi.org/10.3389/fmars.2020.581790>.

- 414 Bibby, T. S., & Moore, C. M. (2011). Silicate:nitrate ratios of upwelled waters control the
415 phytoplankton community sustained by mesoscale eddies in sub-tropical North
416 Atlantic and Pacific. *Biogeosciences*, 8(3), 657–666. [https://doi.org/10.5194/bg-8-657-](https://doi.org/10.5194/bg-8-657-2011)
417 2011
- 418 Bopp, L., Aumont, O., Cadule, P., Alvain, S., & Gehlen, M. (2005). Response of diatoms
419 distribution to global warming and potential implications: A global model study,
420 *Geophys. Res. Lett.*, 32, L19606, doi:10.1029/2005GL023653, 2005
- 421 Børsheim, K.Y., Bratbak, G. (1987). Cell volume to cell carbon conversion factors for a
422 bacterivorous *Monas* sp. enriched from seawater. *Mar. Ecol. Prog. Ser.* 36, 171–175.
- 423 Brzezinski, M.A. (1985). The Si:C:N ratio of marine diatoms: interspecific variability and
424 the effect of some environmental variables. *J. Phycol.* 21,
425 347–357. <https://doi.org/10.1111/j.0022-3646.198.00347.x>.
- 426 Buitenhuis, E.T., Li, W.K.W., Vaulot, D., Lomas, M.W., Landry, M.R., Partensky, F., Karl,
427 D.M., Ulloa, O., Campbell, L., Jacquet, S., Lantoine, F., Chavez, F., MacIas, D.,
428 Gosselin, M., McManus, G.B. (2012). Picophytoplankton biomass distribution in the
429 global ocean. *Earth Syst. Sci. Data* 4, 37–46. <https://doi.org/10.5194/essd-4-37-2012>
- 430 Calbet, A., & Landry, M. R. (2004). Phytoplankton growth, microzooplankton grazing, and
431 carbon cycling in marine systems. *Limnology and Oceanography*, 49(1), 51–57.
432 <https://doi.org/10.4319/lo.2004.49.1.0051>
- 433 Campbell, L. (2001). Flow Cytometric Analysis of Autotrophic Picoplankton, *Methods in*
434 *Microbiology*. Academic Press, pp. 317–343.
- 435 Carter, R. A., McMurray, H. F., Largier, J. L., McMurray, H. F., & Thermocline, J. L. L.
436 (1987). Thermocline characteristics and phytoplankton dynamics in Agulhas Bank
437 waters. *South African Journal of Marine Science*, 5(1), 327–336.
438 <https://doi.org/10.2989/025776187784522306>.
- 439 Carvalho, F., Kohut, J., Oliver, M.J. & Schofield, O. (2017). Defining the
440 ecologically relevant mixed-layer depth for Antarctica’s coastal seas. *Geophys.*
441 *Res. Lett.* 44, 338–345. <https://doi.org/10.1002/2016GL071205>.

- 442 Chen, T.Y., Lai, C.C., Tai, J.H., Ko, C.Y., Shiah, F.K. (2021). Diel to Seasonal Variation of
443 Picoplankton in the Tropical South China Sea. *Front. Mar. Sci.* 8, 1–12.
444 <https://doi.org/10.3389/fmars.2021.732017>.
- 445 Chisholm, S. W., Olson, R. J., Zettler, E. R., Goericke, R., Waterbury, J. B. & Welschmeyer,
446 N. A. (1988). A novel free-living prochlorophyte abundant in the oceanic euphotic
447 zone. *Nature*, 334, 340–343.
- 448 Daneri, G., Lizárraga, L., Montero, P., González, H.E., Tapia, F.J. (2012). Wind forcing and
449 short-term variability of phytoplankton and heterotrophic bacterioplankton in the
450 coastal zone of the Concepcion upwelling system (Central Chile). *Prog. Ocea.*, 92-96.
- 451 Dutkiewicz, S., Scott, J. R. & Follows, M. J. (2013). Winners and losers: ecological and
452 biogeochemical changes in a warming ocean. *Glob. Biogeochem. Cycles* 27,
453 463-477.
- 454 Field, C. B., Behrenfeld, M. J., Randerson, J. T., & Falkowski, P. (1998). Primary production
455 of the biosphere: Integrating terrestrial and oceanic components. *Science*, 281(5374),
456 237–240. <https://doi.org/10.1126/science.281.5374.237>
- 457 Flander-Putrlle, V., Francé, J., & Mozetič, P. (2021). Phytoplankton pigments reveal size
458 structure and interannual variability of the coastal phytoplankton community (Adriatic
459 Sea). *Water (Switzerland)*, 14(1). <https://doi.org/10.3390/w14010023>
- 460 Flombaum, P., Wang, W.L., Primeau, F.W. et al. (2020). Global picophytoplankton niche
461 partitioning predicts overall positive response to ocean warming. *Nat. Geosci.* 13, 116–
462 120. <https://doi.org/10.1038/s41561-019-0524-2>
- 463 Henson, S.A., Cael, B.B., Allen, S.R. & Dutkiewicz, S. (2021). Future phytoplankton
464 diversity in a changing climate. *Nat Commun* 12, 5372.
465 <https://doi.org/10.1038/s41467-021-25699-w>
- 466 Huggett, J. A., Noyon, M., Carstensen, J., & Walker, D. R. (2023). Patterns in the plankton –
467 Spatial distribution and long-term variability of copepods on the Agulhas Bank. *Deep-
468 Sea Research Part II: Topical Studies in Oceanography*, 208,
469 105265. <https://doi.org/10.1016/j.dsr2.2023.105265>
- 470 Hutchings, L., van der Lingen, C.D., Shannon, L.J., Crawford, R.J.M., Verheye, H.M.S.,
471 Bartholomae, C.H., van der Plas, A.K., Louw, D., Kreiner, A., Ostrowski, M., Fidel,

472 Q., Barlow, R.G., Lamont, T., Coetzee, J., Shillington, F., Veitch, J., Currie, J.C., &
473 Monteiro, P.M.S. (2009). The Benguela Current: an ecosystem of four components.
474 *Prog. Oceanogr.* 83, 15–32. <http://dx.doi.org/10.1016/j.pocean.2009.07.046>.

475 Hydes, D. J., Aoyama, M., Aminot, A., Bakker, K., Becker, S., Coverly, S., et al. (2010).
476 Determination of dissolved nutrients (N, P, Si) in seawater with high precision and
477 inter-comparability using gas-segmented continuous flow analysers, In: *The GO-SHIP*
478 *repeat hydrography manual: A collection of expert reports and guidelines*. IOCCP
479 report No. 14. ICPO publication series No. 134.

480 Jackson, J. M., Rainville, L., Roberts, M. J., McQuaid, C. D., & Lutjeharms, J. R. E. (2012).
481 Mesoscale bio-physical interactions between the Agulhas Current and the Agulhas
482 Bank, South Africa. *Continental Shelf Research*, 49,
483 10–24. <https://doi.org/10.1016/j.csr.2012.09.005>

484 Lamont, T., Brewin, R. J. W., & Barlow, R. G. (2018). Seasonal variation in remotely-sensed
485 phytoplankton size structure around southern Africa. *Remote Sensing of Environment*,
486 204, 617–631. <https://doi.org/10.1016/j.rse.2017.09.038>

487 Liang, Y., Zhang, Y., Zhang, Y., Luo, T., Rivkin, R. B. and Jiao, N. (2017). Distributions and
488 relationships of virio- and picoplankton in the epi-, meso- and bathypelagic zones of
489 the Western Pacific Ocean. *FEMS Microbiology Ecology* 93(2), fiw238

490 Liu, H., Probert, I., Uitz, J., Claustre, H., Aris-Brosou, S., Frada, M., et al. (2009). Extreme
491 diversity in noncalcifying haptophytes explains a major pigment paradox in open
492 oceans. *Proceedings of the National Academy of Sciences of the United States of*
493 *America*, 106(31), 12803–12808. <https://doi.org/10.1073/pnas.0905841106>

494 Lomas, M. W., Moran, S. B., Casey, J. R., Bell, D. W., Tiahlo, M., Whitefield, J., et al.
495 (2012). Spatial and seasonal variability of primary production on the Eastern Bering
496 Sea shelf. *Deep-Sea Research Part II: Topical Studies in Oceanography*, 65–70,
497 126–140. <https://doi.org/10.1016/j.dsr2.2012.02.010>

498 Malan, N., Backeberg, B., Biastoch, A., Durgadoo, J. V., Samuelsen, A., Reason, C., &
499 Hermes, J. (2018). Agulhas Current meanders facilitate shelf-slope exchange on the
500 Eastern Agulhas Bank. *Journal Geophysical Research: Oceans*, 123, 4762–4778.
501 <https://doi.org/10.1029/2017JC013602>

502 Marañón, E. (2015). Cell size as a key determinant of phytoplankton metabolism and
503 community structure. *Ann Rev Mar Sci.* 7:241-64. doi: 10.1146/annurev-marine-
504 010814- 015955. Epub 2014 Jul 25. PMID: 25062405.

505 Marie, D., Partensky, F., Jacquet, S., Vaultot, D. (1997). Enumeration and cell cycle analysis
506 of natural populations of marine picoplankton by flow cytometry using the nucleic
507 acid stain SYBR Green I. *Appl. Environ. Microbiol.* 63, 186–193.

508 Mayers, K. M. J., Poulton, A. J., Daniels, C. J., Wells, S. R., Woodward, E. M. S., Tarran, G.
509 A., et al. (2019). Growth and mortality of coccolithophores during spring in a
510 temperate Shelf Sea (Celtic Sea, April 2015). *Progress in Oceanography*, 177,
511 101928. <https://doi.org/10.1016/j.pocean.2018.02.024>

512 Mazwane, S. L., Poulton, A. J., Hickman, A. E., Jebri, F., Jacobs, Z., Roberts, M., & Noyon,
513 M. (2022). Spatial and temporal variability of Net Primary Production on the Agulhas
514 Bank, 1998–2018. *Deep-Sea Research Part II: Topical Studies in Oceanography*, 199,
515 105079. <https://doi.org/10.1016/j.dsr2.2022.105079>

516 Mena, C., Reglero, P., Hidalgo, M., Sintes, E., Santiago, R., Martín, M., Moyà, G. & Balbín,
517 R. (2019). Phytoplankton Community Structure Is Driven by Stratification in the
518 Oligotrophic Mediterranean Sea. *Front. Microbiol.* 10:1698.
519 doi:10.3389/fmicb.2019.01698

520 Mitra, A., Caron, D.A., Faure, E., Flynn, K.J., Gonçalves Leles, S., Hansen, P.J. et al. (2023).
521 The Mixoplankton database (MDB). Zenodo. <https://doi.org/10.5281/zenodo.7560583>

522 Moore, C. M., Suggett, D., Holligan, P. M., Sharples, J., Abraham, E. R., Lucas, M. I., et al.
523 (2003). Physical controls on phytoplankton physiology and production at a shelf sea
524 front: A fast repetition-rate fluorometer based field study. *Marine Ecology Progress*
525 *Series*, 259, 29–45. <https://doi.org/10.3354/meps259029>

526 Moore, C.M., Mills, M.M., Achterberg, E.P., Geider, R.J., LaRoche, J., Lucas, M.I.,
527 McDonagh, E.L., Pan, X., Poulton, A.J., Rijkenberg, M.J.A., Suggett, D.J., Ussher, S.
528 J. & Woodward, E.M.S. (2009). Large-scale distribution of Atlantic nitrogen
529 fixation controlled by iron availability. *Nat. Geosci.* 2, 867–871.
530 <https://doi.org/10.1038/ngeo667>.

531 Moran, M. A., 2015. The global ocean microbiome. *Science*.350(6225), aac8455.

- 532 Noyon, M. (2019). Oceanographic Survey of the Eastern and Central Agulhas Bank (South
533 Africa). Port Elizabeth.
- 534 Noyon, M., Poulton, A.J., Asdar, S., Weitz, R., Giering, S.L.C. (2022). Mesozooplankton
535 community distribution on the Agulhas Bank in autumn: Size structure and production.
536 Deep. Res. Part II Top. Stud. Oceanogr. 195,
537 105015. <https://doi.org/10.1016/j.dsr2.2021.105015>
- 538 Pauly, D., Christensen, V., Guénette, S., Pitcher, T. J., Sumaila, U. R., Walters, C. J., et al.
539 (2002). Towards sustainability in world fisheries. *Nature*, 418 (6898), 689–695.
540 <https://doi.org/10.1038/nature01017>
- 541 Poulton, A. J., Mazwane, S. L., Godfrey, B., Carvalho, F., Mawji, E., Wihsgott, J. U., &
542 Noyon, M. (2022). Primary production dynamics on the Agulhas Bank in autumn.
543 Deep-Sea Research Part II: Topical Studies in
544 Oceanography, 203. <https://doi.org/10.1016/j.dsr2.2022.105153>
- 545 Poulton, A. J., Young, J. R., Bates, N. R., & Balch, W. M. (2011). Biometry of detached
546 *Emiliania huxleyi* coccoliths along the Patagonian Shelf. *Marine Ecology Progress*
547 *Series*, 443, 1–17. <https://doi.org/10.3354/meps09445>
- 548 Probyn, T. A., Mitchell-Innes, B. A., Brown, P. C., Hutchings, L., & Carter, R. A. (1994). A
549 review of primary production and related processes on the Agulhas Bank. *South*
550 *African Journal of Science*, 90, 166–173.
- 551 Rajaneesh, K. M., Mitbavkar, S., Anil, A. C., & Sawant, S. S. (2015). *Synechococcus* as an
552 indicator of trophic status in the Cochin backwaters, west coast of India. *Ecological*
553 *Indicators*, 55, 118-130.
- 554 Rajaneesh, K. M., Mitbavkar, S., & Anil, A. C. (2017). Influence of short-term hydrographic
555 variations during the north-east monsoon on picophytoplankton community structure
556 in the eastern Arabian Sea. *Continental Shelf Research*, 146, 28–36.
557 <https://doi.org/10.1016/j.csr.2017.08.008>
- 558 Redfield, A.C. (1958). The biological control of chemical factors in the environment. *Am.*
559 *Sci.* 46, 205–221. <https://www.jstor.org/stable/27827150>.
- 560 Safi, K. A., Rodríguez, A. G., Hall, J. A., & Pinkerton, M. H. (2023). Phytoplankton
561 dynamics, growth and microzooplankton grazing across the subtropical frontal zone,

562 east of New Zealand. *Deep-Sea Research Part II: Topical Studies in Oceanography*,
563 208(January). <https://doi.org/10.1016/j.dsr2.2023.105271>

564 Scanlan D.J., Ostrowski, M., Mazard, S., Dufresne, A., Garczarek, L., Hess, W.R., Post, A.F.,
565 Hagemann, M., Paulsen, I., Partensky F. (2009). Ecological genomics of marine
566 picocyanobacteria; *Microbiology and molecular biology reviews* 73(2), 249-299

567 Sieburth, J. (1979). *Sea microbes*. Oxford University Press New York

568 Sonnekus, M.J. (2020). *Phytoplankton of the Southern Agulhas Large Marine Ecosystem*
569 (sACLME). PhD Thesis, Nelson Mandela University, Gqeberha (formerly Port
570 Elizabeth), South Africa. Pp1-262

571 Tarran, G. A., Heywood, J. L., & Zubkov, M. V. (2006). Latitudinal changes in the standing
572 stocks of nano- and picoeukaryotic phytoplankton in the Atlantic Ocean. *Deep-Sea*
573 *Research Part II: Topical Studies in Oceanography*, 53(14–16), 1516–1529.
574 <https://doi.org/10.1016/j.dsr2.2006.05.004>

575 Van Dongen-Vogels, V., Seymour, J.R., Middleton, J.F., Mitchell, J.G., Seuront, L. (2012).
576 Shifts in picophytoplankton community structure influenced by changing upwelling
577 conditions. *Estuar. Coast. Shelf Sci.* 109, 81–90.
578 <https://doi.org/10.1016/j.ecss.2012.05.026>

579 Van Dongen-Vogels, V., Seymour, J.R., Middleton, J.F., Mitchell, J.G., Seuront, L. (2011).
580 Influence of local physical events on picophytoplankton spatial and temporal dynamics
581 in South Australian continental shelf waters. *J. Plankton Res.* 33, 1825–
582 1841. <https://doi.org/10.1093/plankt/fbr077>

583 Wang, F., Wei, Y., Zhang, G., Zhang, L., & Sun, J. (2022). Picophytoplankton in the West
584 Pacific Ocean: A Snapshot. *Frontiers in Microbiology*, 13, 1–13.
585 <https://doi.org/10.3389/fmicb.2022.811227>

586 Waterbury, J. B., Watson, S. W., Guillard, R. R. L. et al. (1979) Widespread occurrence of a
587 unicellular, marine planktonic, cyano- bacterium. *Nature*, 277, 293–294. Wei, Y.,
588 Huang, D., Zhang, G., Zhao, Y. & Sun, J. (2020). Biogeographic variations of
589 picophytoplankton in three contrasting seas: The Bay of Bengal, South China Sea and
590 western Pacific Ocean. *Aquat. Microb. Ecol.* 84, 91–103.
591 <https://doi.org/10.3354/ame01928>

- 592 Wei, Y., Huang, D., Zhang, G., Zhao, Y., & Sun, J. (2020). Biogeographic variations of
593 picophytoplankton in three contrasting seas: The Bay of Bengal, South China Sea and
594 western Pacific Ocean. *Aquatic Microbial Ecology*, 84(1), 91–
595 103. <https://doi.org/10.3354/ame01928>
- 596 Worden, A. Z. (2006). Picoeukaryote diversity in coastal waters of the Pacific Ocean.
597 *Aquatic Microbial Ecology*, 43(2), 165-175.

Table 1. Results of Principal Component Analysis (PCA), including eigenvalues and Pearson correlation coefficients for the relationships between PC scores, hydrographic variables, and absolute and relative phytoplankton group biomass (n = 28). *p < 0.05; **p < 0.01; ***p < 0.005.

<i>Hydrography</i>	SST	\bar{E}_{SML}	N ² max.	SML NO ₃	SML Si(OH) ₄
PC-1	-1.4 (-0.92***)	0.44 (0.29)	-0.39 (-0.26)	1.30 (0.85***)	1.06 (0.70***)
PC-2	-0.28 (-0.19)	-1.04 (-0.68***)	1.14 (0.75***)	-0.26 (-0.17)	0.79 (0.52**)
	PRO	SYN	PICO	NANO	CRYPTO
<i>Absolute Biomass</i>					
PC-1	-0.36	-0.41*	-0.45*	-0.27	-0.28
PC-2	-0.09	0.2	-0.004	-0.06	0.06
<i>Relative Biomass</i>					
PC-1	-0.02	-0.10	-0.1	0.29	-0.32
PC-2	-0.26	0.17	-0.07	0.03	0.16

Figure1.

Figure 1. Phytoplankton biomass distribution on the Agulhas Bank in autumn. (a) Surface calibrated-fluorescence FChl (mg m^{-3}) superimposed on an 8-day composite (28/2/2019 – 06/3/2019) of satellite Chl (4 km Ocean Colour Climate Change Initiative (OCCI) data); euphotic zone integrated biomass (g C m^{-2}) of each group (b) PRO, (c) SYN, (d) PICO, (E) NANO, and (F) CRYPTO. Bathymetry marks the 200 m isobath.

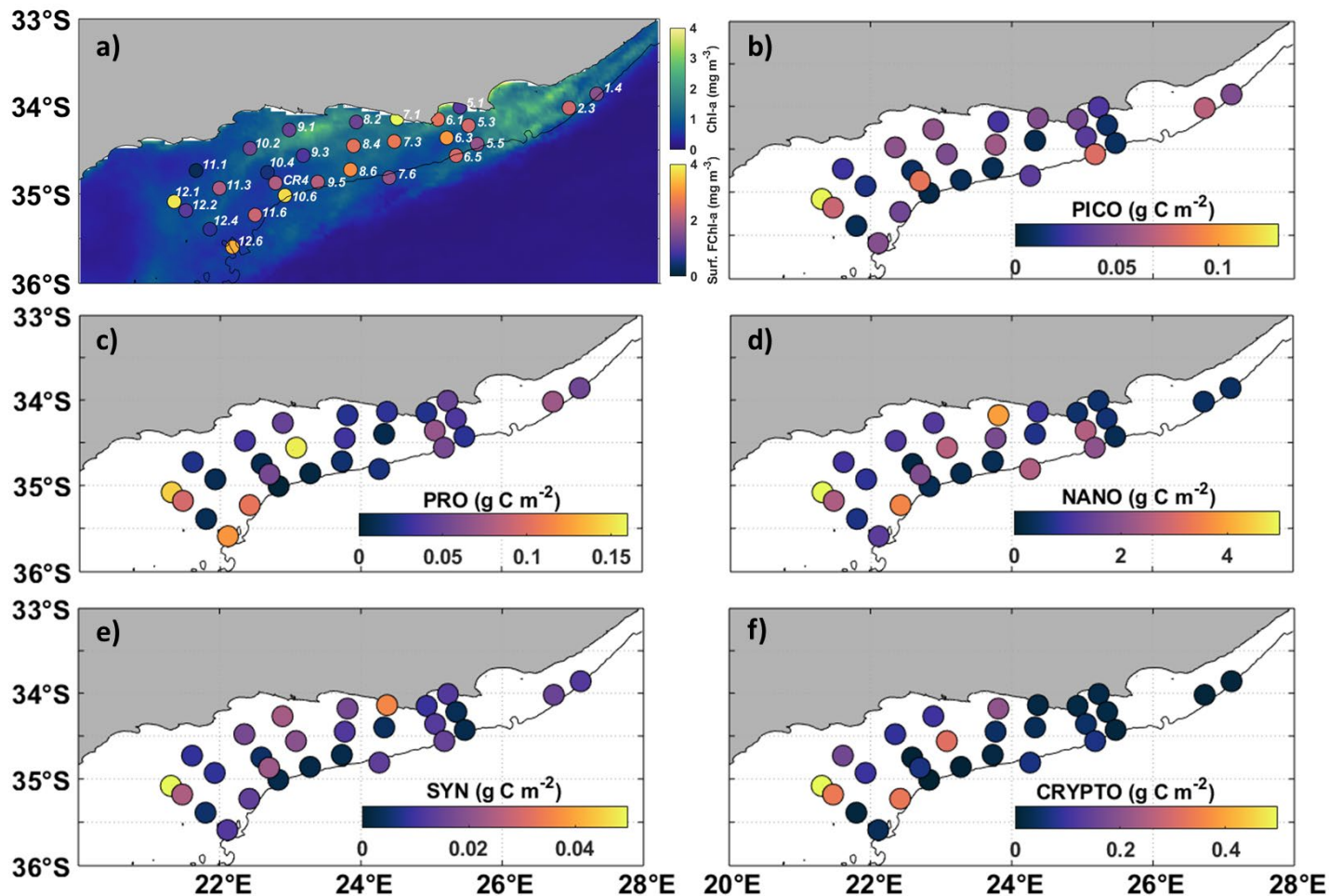


Figure2.

Figure 2. Boxplots of biomass (g C m^{-3}) in surface waters, the sub-surface chlorophyll maximum (SCM) and at the base of the euphotic depth (Z_{eu}) for each group (a) PRO, (b) SYN, (c) PICO, (d) NANO, and (e) CRYPTO. The boxplots indicate values of median (solid horizontal line), 25th and 75th percentiles (box ranges), confident intervals (whiskers), and outliers (black dots).

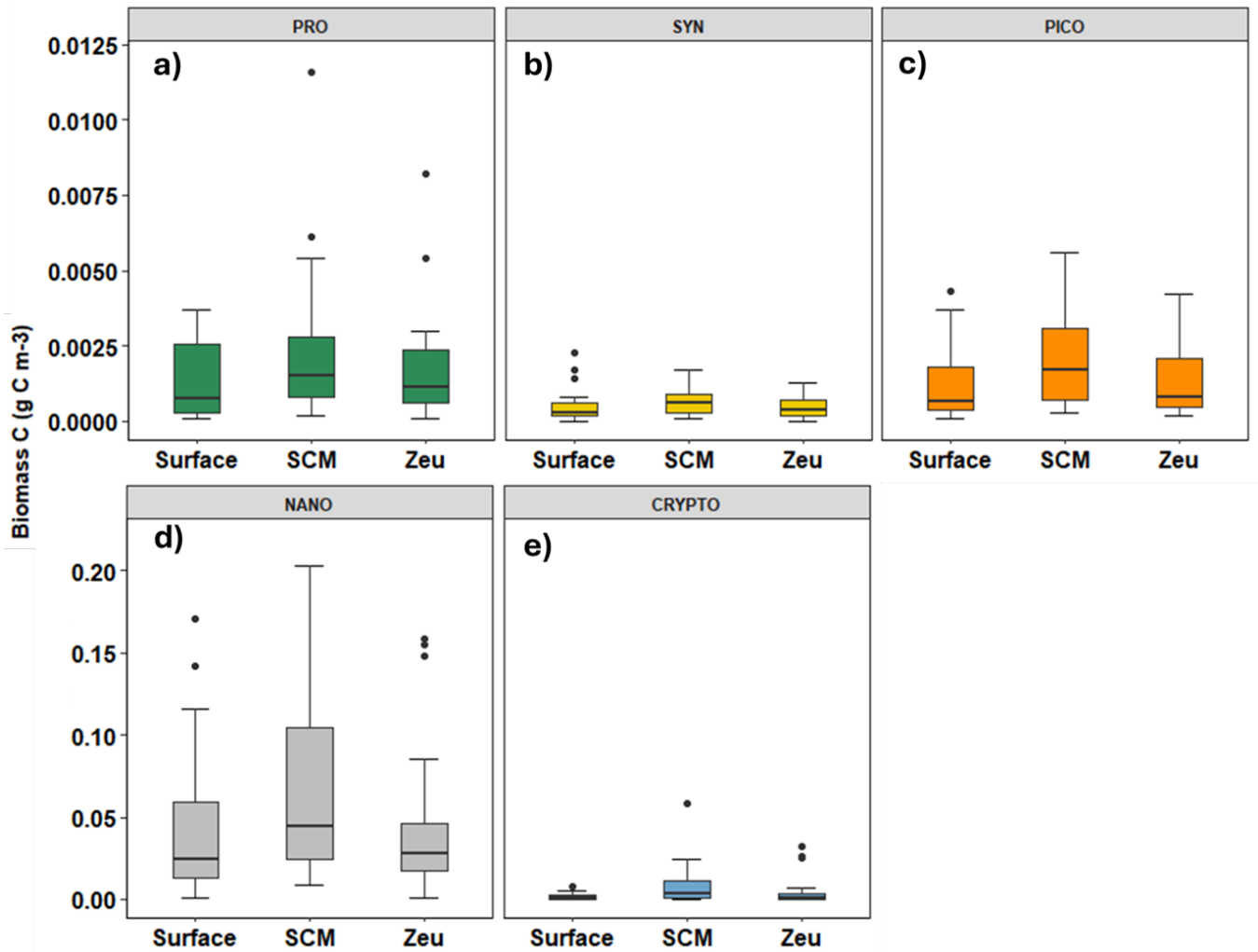
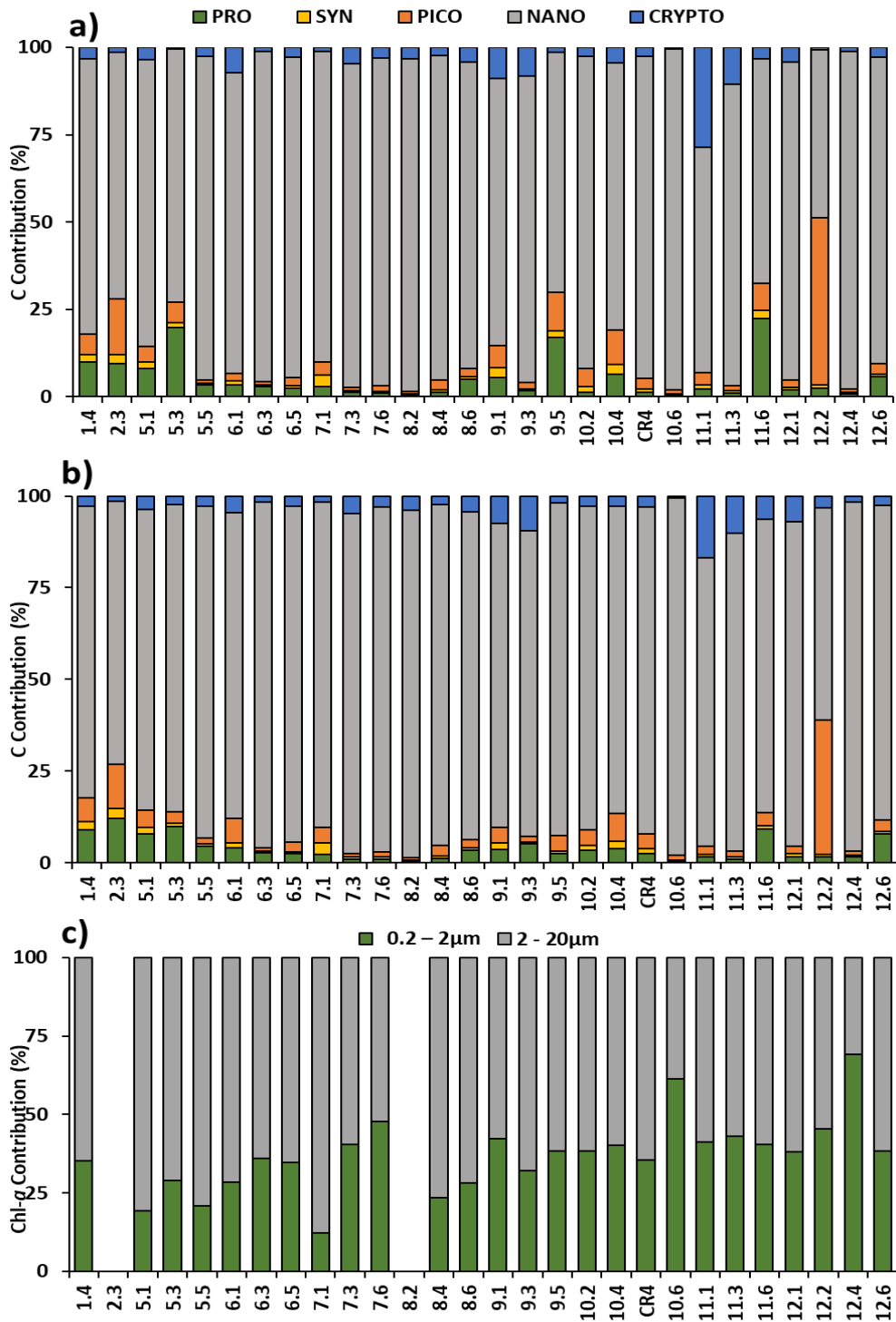


Figure3.

Figure 3. Phytoplankton group contributions (%) to total carbon biomass for surface waters (a) and integrated euphotic zone (b), and for integrated size fractionated Chl (c). PRO, SYN, PICO, NANO and CRYPTO. (c) size fractionated Chl (Poulton et al., 2022) for picoplankton (0.2-2 μm) and nanoplankton (2-20 μm) in the euphotic zone.



1 **Nanoplankton dominate autumn biomass on the Agulhas Bank**

2

3 **Sixolile L. Mazwane¹, Alex J. Poulton², Margaux Noyon¹, Emma Roche³, Mike J.**
4 **Roberts^{1,4}**

5

6 ¹Department of Oceanography and Institute for Coastal and Marine Research, Nelson Mandela
7 University, Port Elizabeth 6001, South Africa.

8 ²The Lyell Centre for Earth and Marine Science, Heriot-Watt University, Riccarton Campus,
9 Edinburgh, EH14 4AP, UK.

10 ³Department of Biological Sciences and Marine Research Institute, University of Cape Town, Cape
11 Town 7701, South Africa

12 ⁴School of Ocean and Earth Sciences, University of Southampton, Southampton, United Kingdom

13

14 Corresponding author: Sixolile Mazwane (Smazwane46@gmail.com)

15

16 **ORCID IDs**

17 Sixolile Mazwane (0000-0001-8707-3111)

18 Alex Poulton (0000-0002-5149-6961)

19 Margaux Noyon (0000-0002-0761-4174)

20 Emma Roche (0000-0001-9514-9788)

21 Mike Roberts (0000-0003-3231-180X)

22

23 **Key points:**

- 24 • Nanoplankton dominate carbon (>80% total) biomass in autumn on the Agulhas
25 Bank.
- 26 • Nanoplankton dominance highlights micro-zooplankton grazing for trophic transfer.
- 27 • Nanoplankton and micro-zooplankton key to productive Agulhas Bank ecosystems.

28

29 **Abstract**

30 Autumn productivity is key to the large marine ecosystems of the Agulhas Bank, which support
31 numerous economically important regional fisheries. Despite such importance, data is sparse
32 on plankton composition in terms of primary or secondary producers, or on trophic transfer.
33 While investigating autumn plankton composition we found that nanophytoplankton (2-20
34 μm) dominated carbon stocks, with lower contributions from picophytoplankton (<2
35 μm) and microphytoplankton (>20 μm). While picoplankton biomass exhibited a
36 relationship with warm nutrient poor waters, nanoplankton showed no clear relationship
37 to environmental parameters. The dominance of nanophytoplankton biomass on the Agulhas
38 Bank highlights a critical role for micro-zooplankton grazing as a trophic transfer between
39 these small plankton, meso-zooplankton and the higher trophic levels that make the bank so
40 important for regional fisheries. Outside of localized coastal upwelling on the Agulhas Bank,
41 this study highlights a significant role for nanoplankton and micro-zooplankton in supporting
42 the bank's large marine ecosystems.

43 **Plain Language Summary**

44 Phytoplankton support productive marine ecosystems through provision of primary
45 production and biomass, with their size-structure determining the efficiency of transfer of
46 energy through the ecosystem. Dominance of small phytoplankton (<20 μm) leads to longer
47 food chains and transfer of energy and biomass to higher trophic levels. Observations of
48 the Agulhas Bank plankton community in autumn, a period of important primary
49 productivity for the region, found a dominance of small nanoplankton (2-20 μm) in terms
50 of biomass. Nanoplankton dominance has important implications for how the Agulhas
51 Bank ecosystem function, highlighting a significant role for micro-zooplankton. The
52 Agulhas Bank is a data sparse environment currently no research on micro-zooplankton
53 has focused on the Agulhas Bank and this is an obvious important group to study further
54 to better understand how the marine ecosystem supports the key regional fisheries that rely
55 on this area.

56

57

58

59

60 1. Introduction

61

62 Phytoplankton support marine food webs and the carbon cycle, accounting for ~50% of global
63 net primary production (Field et al., 1998). Plankton size structure constrains ecosystem
64 productivity (Marañón, 2015), determining the proportion of production passed to higher
65 trophic levels, recycled or exported to the deep sea (Acevedo-Trejos et al., 2015).
66 Phytoplankton may be split into different size categories (Sieburth, 1979): picoplankton (cell
67 diameters 0.2-2 μm), nanoplankton (2-20 μm) and microplankton ($>20 \mu\text{m}$). The small cell
68 diameters of pico- and nano-plankton are not grazed by meso-zooplankton ($>200 \mu\text{m}$) (Huggett
69 et al., 2023, Mitra et al., 2023), and instead are predated by micro-zooplankton (20-200 μm)
70 who then may be grazed by larger zooplankton.

71 Picoplankton are made up of the cyanobacteria *Prochlorococcus* (PRO) and *Synechococcus*
72 (SYN) (Waterbury et al., 1979; Chisholm et al., 1988; Rajaneesh et al., 2017), and a diverse set
73 of pico-eukaryotes (PICO) (Worden, 2006). SYN and PICO favor light and nutrient rich waters
74 (Moore et al., 2003; Rajaneesh et al., 2015). Nanoplankton (NANO, 2-20 μm) include a diverse
75 number of taxa, including Haptophytes, Pelagophytes, and Cryptophytes (CRYPTO) (Flander-
76 Putrle et al., 2021), with haptophytes often dominating (Liu et al., 2009). Larger microplankton
77 ($>20 \mu\text{m}$) are most frequently associated with diatoms and dinoflagellates (Rajaneesh et al.,
78 2017; Lamont et al., 2018).

79 PRO and SYN have overlapping ecological niches of warm low-nutrient waters and
80 may contribute up to 80% of phytoplankton biomass and productivity (Scanlan et al., 2009;
81 Wang et al., 2022), despite their relatively small size (0.5-0.7 μm and 0.7-1.2 μm ,
82 respectively) and cell carbon content (Tarran et al., 2006). PICO are typically less abundant
83 than PRO or SYN by at least an order of magnitude (Flombaum et al., 2020), though
84 they contribute more to biomass due to their larger cell size (0.2-3 μm) and carbon content
85 (Moran, 2015).

86 Shelf seas make a disproportional contribution to primary production compared to their areal
87 extent (Field et al., 1998), supporting ~ 90% of economically important fisheries (Pauly et al.,
88 2002). Shelf seas are often regarded as microplankton dominated, though little is known of the
89 smaller plankton in these systems (van Dongen-Vogels et al., 2011, 2012; Daneri et al., 2012).

90

91 The Agulhas Bank (AB) is a moderately productive shelf (Mazwane et al., 2022) that supports
92 complex trophic structures and numerous commercially harvested marine resources (Hutchings
93 et al., 2009; Lamont et al., 2018). Analysis of satellite and pigment data from the AB has
94 highlighted microplankton dominance in inner shelf waters, with nanoplankton in the adjacent
95 ocean (Barlow et al., 2010; Lamont et al., 2018; Sonnekus, 2022), though such studies have
96 focused on the eastern AB rather than the wider bank.

97 To explore the gap in knowledge of the AB plankton in terms of pico- and nano-plankton, we
98 undertook flow cytometry (Marie et al., 1997; van Dongen-Vogels et al., 2011) of the small
99 phytoplankton (<20 μm) during an autumn (2019) cruise (Figure 1a). Our objectives were to
100 determine the (1) pico- and nano-plankton composition and distribution, (2) contribution of
101 these groupings to carbon biomass, and (3) explore whether variability in composition and
102 biomass were related to prevailing hydrographic gradients.

103 **2. Material and Methods**

104 **2.1. Sampling**

105 Sampling occurred on the AB onboard the *RV Ellen Khuzwayo* (cruise EK188, Noyon
106 (2019), 21 March to 2 April 2019; $n = 28$) (Figure 1a). A Seabird 911+ V2 CTD system
107 with rosette sampler was deployed, with water samples collected using 8 L Niskin bottles
108 (OTE: Ocean Test Equipment), and sampling depths determined from temperature and
109 fluorescence (WET Labs) profiles. Processing and calibration of CTD data followed
110 standard procedures (see Noyon, 2019).

111 A CTD-mounted quantum PAR sensor (LiCor Inc., USA) determined the underwater light
112 field and vertical attenuation coefficient of PAR (K_d , m^{-1}), with the depth of the euphotic zone
113 as the depth that 1% surface irradiance penetrates (Poulton et al. 2022). Sea-surface
114 Temperature (SST) was measured *in-situ* using a CTD-mounted temperature sensor. The
115 surface mixed layer (SML) was determined as the depth of the maximum buoyancy
116 frequency (Carvalho et al., 2017), with the maximum (N^2 max.) value used as a
117 stratification index (Poulton et al., 2022). Average SML irradiance (\bar{E}_{SML}) was determined
118 using a combination of K_d and SML (Poulton et al., 2011).

119

120

121 2.2. Flow Cytometry

122

123 Flow cytometry samples were collected from 4-5 depths, including sub-surface waters (~3
124 m), the beginning, maximum and lower limit of the fluorescence maximum, and below
125 the strongest temperature gradient (thermocline). Seawater samples were pre-filtered through
126 200 μm mesh to remove zooplankton, and 2 mL triplicate aliquots were fixed in
127 0.25% glutaraldehyde (v/v, final concentration), flash frozen and stored (-80°C) prior to
128 analysis.

129 Cell abundances (after Marie et al., 1997; van Dongen-Vogels et al., 2011) were determined
130 on a LSRII (Becton Dickinson) flow cytometer with a 488-nm excitation laser and standard
131 filter set (Campbell, 2001). FlowJo® software calculated PRO and SYN cell abundances.
132 PICO, NANO and CRYPTO were measured through their respective signals emitted in
133 orange (PE: 585/42 band pass) versus red (PC: 661/16 band pass) wavelengths. SYN
134 abundance was distinguished from PICO and PRO through higher (per cell)
135 phycoerythrin signals. The samples were thawed at room temperature and transferred to
136 glass tubes and analyzed. Data were acquired at a medium flow rate with a threshold of
137 ~10,000 events per run and the LSRII was calibrated daily using 3.0 μm Rainbow beads
138 (Spherotech).

139 Cell abundances (cells mL^{-1}) were calculated from the mean of the triplicate samples, with
140 relative standard deviations between triplicates ranging from 1-54% (average: 20%). Cell
141 abundances were converted to cell biomass using literature values (Børsheim and Bratbak,
142 1987; Tarran et al., 2006): 2.7 fmol C cell^{-1} , Prochlorococcus (PRO); 8.58 fmol C cell^{-1} ,
143 Synechococcus (SYN); 36.67 fmol C cell^{-1} for pico-eukaryotes (PICO); 0.26 pmol C cell^{-1} for
144 nanoeukaryotes (NANO); 0.26 pmol C cell^{-1} , for cryptophytes (CRYPTO).

145 For this study, the biomass integrations were calculated for the euphotic depth and MLD (see
146 Table S1). The conversion values were chosen as values previously used for shelf waters
147 rather than the open ocean. For NANO and CRYPTO, we used values from Børsheim and
148 Bratbak (1987). Using Tarran et al. (2006) values would increase the NANO and CRYPTO
149 biomass by 6.8% without changing the biomass patterns.

150

151 **2.3. Size-fractionated Chlorophyll-*a* and Nutrients**

152 Size-fractionated chlorophyll-*a* (Chl) concentrations (mg m^{-3}) were measured on 0.2 L water
153 samples sequentially filtered through 20 μm , 2 μm and 0.2 μm 47-mm NucleoporeTM filters
154 and extracted in 6 mL 90% acetone (Sigma-Aldrich, UK) at 4°C for 18-24 hr (Poulton et al.,
155 2022). Chl fluorescence was measured on a Turner Designs TrilogyTM fluorometer using a
156 non- acidification unit calibrated with solid and pure Chl standards (Sigma-Aldrich, UK).

157 Water samples for macronutrient concentrations were collected into acid-cleaned 50 mL
158 HDPE bottles, which were frozen (-20°C) onboard and kept frozen until analysis (see Poulton
159 et al., 2022). Concentrations ($\mu\text{mol L}^{-1}$) of nitrate + nitrite (NO_3), phosphate (PO_4) and silicic
160 acid ($\text{Si}(\text{OH})_4$) were measured with a SEAL QuAAtro39 auto-analyzer following standard
161 protocols (Becker et al., 2020). Certified reference materials were used daily (KANSO,
162 Japan) and analytical procedures followed International GO-SHIP recommendations (Becker
163 et al., 2020). The typical uncertainty of the analytical results were between 0.5% and 1%, and
164 the limits for detection for NO_3 and PO_4 were $0.02 \mu\text{mol L}^{-1}$, while $\text{Si}(\text{OH})_4$ was always
165 higher than the detection limit ($0.05 \mu\text{mol Si L}^{-1}$). Deficiencies of NO_3 relative to PO_4 and
166 $\text{Si}(\text{OH})_4$ were described relative to the Redfield (1958) ratio, with N^* ($= \text{NO}_3 - (16 \times \text{PO}_4)$;
167 Moore et al., 2009), and relative to the 1:1 ratio of $\text{Si}(\text{OH})_4$ to NO_3 uptake in diatoms
168 (Brzezinski, 1985) through Si^* ($= \text{Si}(\text{OH})_4 - \text{NO}_3$; Bibby and Moore, 2011).

169 **3. Results**

170 **3.1. Agulhas Bank Hydrography**

171 A comprehensive overview of the hydrography of the AB during autumn (2019) is provided
172 by Poulton et al. (2022), with the data included in Supplementary Table S1. SST ranged from
173 $17\text{-}22^{\circ}\text{C}$ (average (\pm standard deviation): $20 (\pm 1)^{\circ}\text{C}$) across the AB, with offshore stations
174 generally showing higher SST (Table S2). SML in autumn showed an east (<10 m) to west
175 (>20 m) deepening (Table S2), with the deepest SML at 27 m (average: $15 (\pm 5)$ m). SML
176 deepening was related to warming of the SML, linked to the westward SST increase (Poulton
177 et al., 2022). No clear or consistent inshore-offshore trends in the SML depth or SST were
178 observed.

179 Euphotic zone depths ranged from 23-53 m (Table S2), with an average of 33 m (± 7 m) and
180 no clear east to west or inshore-offshore trend was observed. ESML indicated that
181 phytoplankton in the SML received irradiances ranging from 26-63% (average: $44 (\pm 10)$ %)

182 of the incidental irradiance (Table S2). An east to west trend was observed, with the
183 irradiance decreasing towards the west as the SML deepened (Table S1, Poulton et al., 2022).

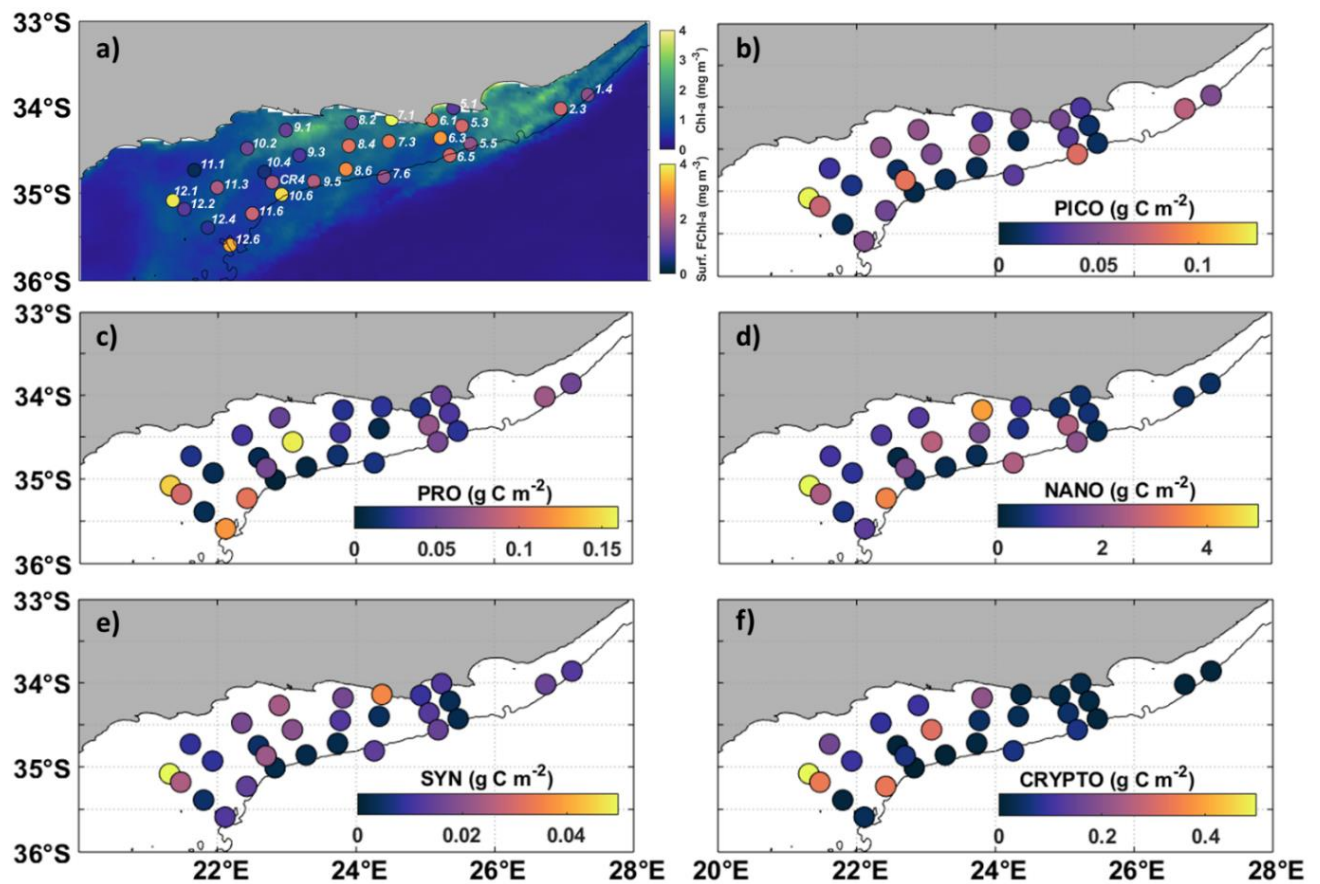
184 The maximum value of the buoyancy frequency (N^2 max.), an indicator of water column
185 stratification, showed an east to west strengthening (Table S2), from values $<4 \times 10^3 \text{ s}^{-2}$ in the
186 east to $\sim 5 \times 10^3 \text{ s}^{-2}$ in the west. Increasing stratification from east to west likely relates to
187 warming of SST, and interactions with the Agulhas Current (Poulton et al., 2022).

188 SML NO_3 ranged from 0.1-6.2 $\mu\text{mol N L}^{-1}$ (average: $1.1 (\pm 1.4) \mu\text{mol N L}^{-1}$), with similar
189 concentrations in the east and west (Table S2). Relative to PO_4 , as indicated by N^* values,
190 NO_3 was always deficient (always negative) relative to Redfield (1958) (Table S2, Poulton et
191 al., 2022). Strong negative values (-6 to -2.5) were related to the subtropical source waters for
192 the AB (Poulton et al., 2022). SML $\text{Si}(\text{OH})_4$ ranged from 0.6-5.1 $\mu\text{mol Si L}^{-1}$ (average: $2.9 (\pm$
193 $1.1) \mu\text{mol Si L}^{-1}$) (Table S2), higher than those found in the subtropical source water and
194 highlighting the role of coastal upwelling in (re)supplying and retaining Si on the AB
195 (Poulton et al., 2022). SML Si^* values were mostly positive on the AB indicating residual
196 silicic acid relative to NO_3 in autumn (Table S2).

197 **3.2. Spatial Distribution of Phytoplankton Biomass**

198 Satellite Chl concentrations ranged from <0.1 - 4.0 mg m^{-3} during autumn, with higher
199 concentrations from east to west (Figure 1a). Surface in-situ Chl ranged from 0.3 - 4.7 mg m^{-3}
200 (average: $2.1 (\pm 1.1) \text{ mg m}^{-3}$) (Figure 1a). Around 46% of sampling stations had Chl $>2 \text{ mg}$
201 m^{-3} and no consistent spatial distribution was observed.

202 In terms of euphotic zone integrated biomass, PRO biomass ranged from 0.002 - 0.16 g C m^{-2}
203 (average: $0.05 (\pm 0.04) \text{ g C m}^{-2}$) (Figure 1b). SYN biomass ranged from 0.002 - 0.05 g C m^{-2}
204 ($0.01 (\pm 0.01)$) and was relatively high ($>0.02 \text{ g C m}^{-2}$) at some of the inshore stations (e.g.,
205 transects 7, 9 and 12), while offshore stations exhibited lower ($<0.01 \text{ g C m}^{-2}$) biomass
206 (Figure 1c). Of all the groups, SYN biomass was the lowest. PICO biomass ranged from
207 0.006 - 0.13 g C m^{-2} (average: $0.04 (\pm 0.03) \text{ g C m}^{-2}$) (Figure 1d). NANO dominated biomass,
208 with estimates ranging from 0.19 - 4.99 g C m^{-2} (average: $1.4 (\pm 1.2) \text{ g C m}^{-2}$) (Figure 1e).
209 NANO biomass was much higher ($>0.3 \text{ g C m}^{-2}$) than the other groups at $\sim 100\%$ of stations.
210 CRYPTO biomass ranged from 0.002 to 1.09 g C m^{-2} (average: $0.12 (\pm 0.22) \text{ g C m}^{-2}$) (Figure
211 1f). No clear spatial patterns were observed for PRO, SYN, PICO, or NANO (Figures 1b-e),
212 though there was a noticeable increase in CRYPTO biomass from east to west (Figure 1f).



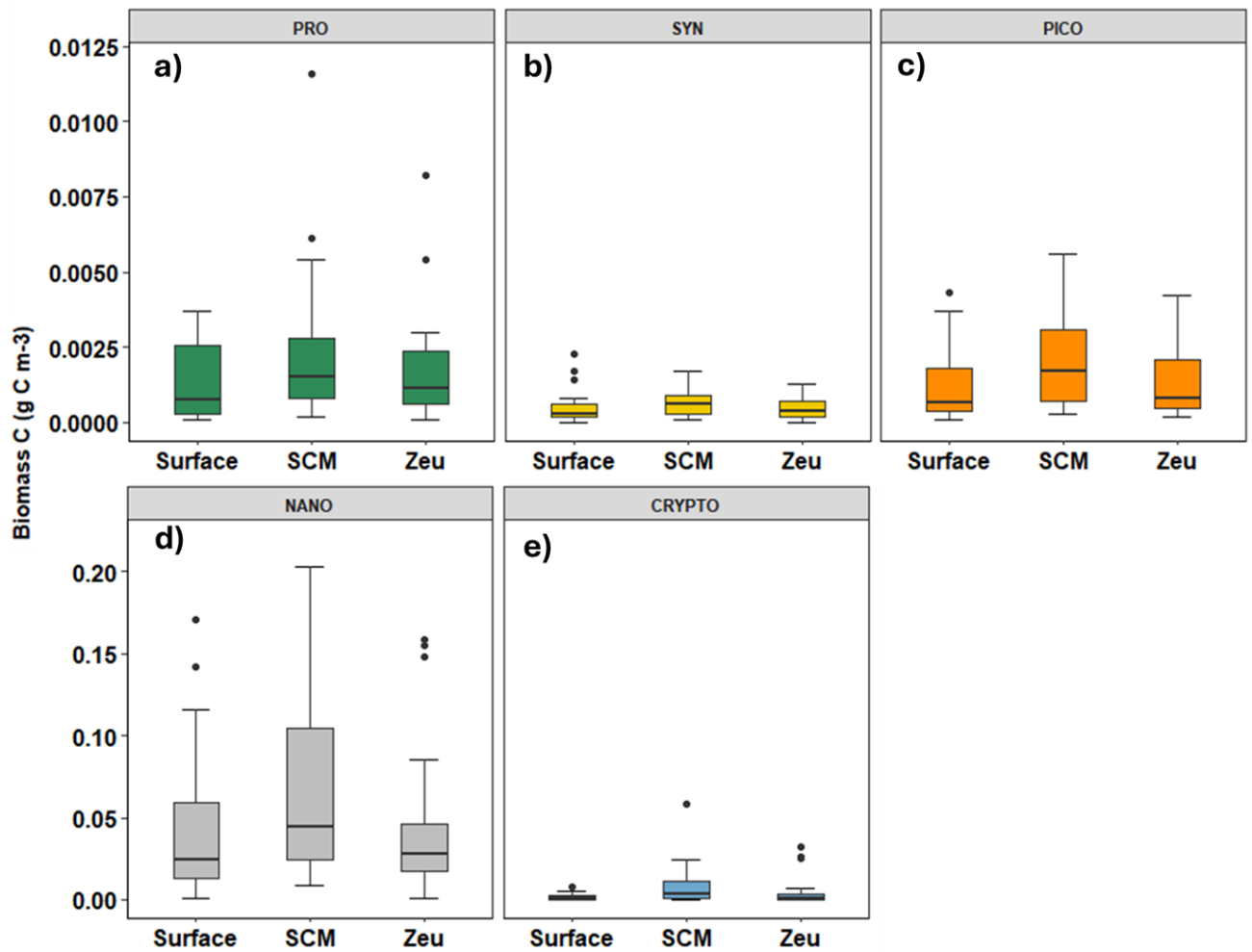
213

214 **Figure 1.** Phytoplankton biomass distribution on the Agulhas Bank in autumn. (a) Surface
 215 calibrated-fluorescence FChl (mg m^{-3}) superimposed on an 8-day composite (28/2/2019 –
 216 06/3/2019) of satellite Chl (4 km Ocean Colour Climate Change Initiative (OCCI) data);
 217 euphotic zone integrated biomass (g C m^{-2}) of each group (b) PRO, (c) SYN, (d) PICO, (E)
 218 NANO, and (F) CRYPTO. Bathymetry marks the 200 m isobath.

219 3.3. Vertical Distribution of Phytoplankton Biomass

220 A sub-surface Chl maximum (SCM) occurred at ~50% of the stations sampled on the AB
 221 (Poulton et al., 2022), ranging in depth from 9 to 41 m and exhibiting no clear spatial pattern
 222 between stations. Generally, the vertical distribution of the different groups in terms of biomass
 223 was variable amongst the sampled stations. The depth of maximum biomass varied throughout
 224 the sampled stations and between the different groups. To examine the vertical distribution of
 225 small phytoplankton biomass, box-and-whisker plots of group biomass concentrations for
 226 surface waters, the SCM and at the base of the euphotic zone (Z_{eu}) are presented in Figure 2.
 227 None of the five groups examined (PRO, SYN, PICO, NANO, CRYPTO) showed any general
 228 depth preferences (Kruskal-Wallis t-tests, $p > 0.05$ for all groups and depth), though the
 229 median biomass for all groups was slightly higher in the SCM than surface or deeper waters

230 (Figures 2a-e). Overall, NANO exhibited higher biomass ($>0.05 \text{ g C m}^{-3}$; Figure 2d) than
 231 all the other groups for the depths examined (Figures 2a-e).



232

233 **Figure 2.** Boxplots of biomass (g C m^{-3}) in surface waters, the sub-surface chlorophyll
 234 maximum (SCM) and at the base of the euphotic depth (Zeu) for each group (a) PRO, (b)
 235 SYN, (c) PICO, (d) NANO, and (e) CRYPTO. The boxplots indicate values of median
 236 (solid horizontal line), 25th and 75th percentiles (box ranges), confident intervals
 237 (whiskers), and outliers (black dots).

238

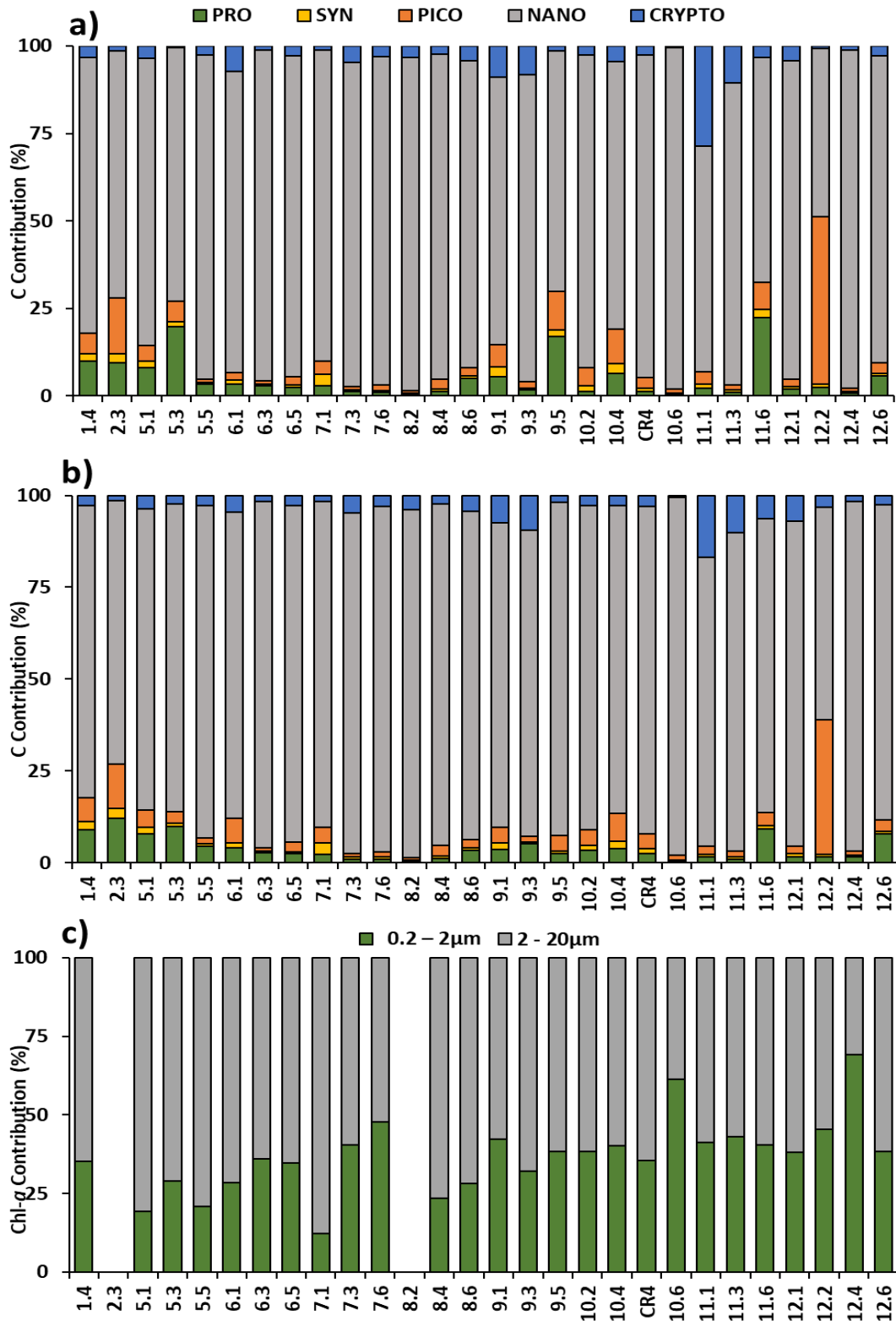
239 3.4. Size-structure of the Phytoplankton Community

240 In surface waters, NANO dominated (average: $85 (\pm 9.9) \%$) community biomass (Figure 3a),
 241 with lower and more similar average contributions from PRO ($5.1 (\pm 5.8) \%$), CRYPTO (4.4
 242 $(\pm 5.4) \%$) and PICO ($4.0 (\pm 3.6) \%$), and much lower contributions from SYN ($1.3 (\pm 0.9)$
 243 $\%$). NANO contributions to surface phytoplankton biomass were always $>70\%$, while PRO

244 contributions were always <15% and only at 6 stations were the contributions >5% (Figure
245 3a). SYN contributions to surface phytoplankton biomass were always <3%, while PICO and
246 CRYPTO were always less than 20% and 15%, respectively.

247 For euphotic zone integrated biomass (Figure 3b), NANO were again dominant ($87 (\pm 5.7)$
248 %), with lower and more similar contributions from CRYPTO ($4.9 (\pm 4.1)$ %), PRO ($3.6 (\pm$
249 $2.8)$ %) and PICO ($3.3 (\pm 2.4)$ %), and SYN contributions $\sim 1\%$ ($1.1 (\pm 0.7)$ %). PRO biomass
250 contribution decreased on average from east to west (5.0 to 2.8%) while CRYPTO
251 contributions increased east to west (2.8 to 6.2%), whereas no clear trend was evident for the
252 other groups. Low (<2%) contributions for SYN were a consistent feature in both surface
253 waters (Figure 3a) and integrated biomass over the euphotic zone on the AB in autumn
254 (Figure 3b).

255 Whether in carbon (Figures 3a & b) or Chl-a biomass (Figure 3c; Poulton et al., 2022), the
256 nanoplankton (2-20 μm) were the dominant size class on the AB in autumn. On average,
257 nanoplankton Chl (NANO+CRYPTO) represented $63.1 (\pm 11.9)$ % of total Chl-a, while
258 picoplankton Chl (PRO+SYN+PICO) represented $36.9 (\pm 11.9)$ % (Figure 3c). Picoplankton
259 contributions to total Chl-a increased east to west (30.4 to 41.0%), while nanoplankton Chl
260 decreased east to west (69.6 to 59.0%). Measurements of microplankton Chl (>20 μm ;
261 Poulton et al., 2022) showed low contributions (<30%) across most of the AB, with few
262 stations characterised by microplankton dominance (not shown).



263

264 **Figure 3.** Phytoplankton group contributions (%) to total carbon biomass for surface waters
 265 (a) and integrated euphotic zone (b), and for integrated size fractionated Chl (c). PRO, SYN,
 266 PICO, NANO and CRYPTO. (c) size fractionated Chl (Poulton et al., 2022) for picoplankton
 267 (0.2-2 µm) and nanoplankton (2-20 µm) in the euphotic zone.

268 **3.5. Phytoplankton Biomass and Agulhas Bank Hydrography**

269 To explore the relationship between environmental conditions and phytoplankton
 270 composition, variability in hydrography (SST, \bar{E}_{SML} , N^2 max., and SML average nutrient
 271 concentrations [NO_3 , $Si(OH)_4$]) was assessed with a Principal Component Analysis (PCA) (R
 272 vegan package). PC1 explained 44% of the variance between stations, while PC2 explained
 273 27% and three next PCs explained less than 15% each. PC1 describes an inverse relationship
 274 between SST and nutrient (NO_3 , $Si(OH)_4$) concentrations (Table 1); warmer waters were
 275 more nutrient poor on the AB. PC2 describes an inverse relationship between stratification
 276 (N^2 max.) and \bar{E}_{SML} (Table 1); with stronger stratification leading to shallower SML and
 277 higher average irradiances.

278 Though PC1 and PC2 reflected the spatial variability in hydrographic conditions across the
 279 AB (see also Poulton et al., 2022), Pearson correlation showed that there was limited co-
 280 variability with phytoplankton biomass or community composition (Table 1). Only the
 281 absolute biomass of PICO and SYN showed (negative) statistically significant ($p < 0.05$)
 282 correlations with PC1; no statistically significant correlations were observed with the biomass
 283 of the other groups present on the AB (Table 1). This highlights higher biomass of PICO and
 284 SYN warmer, more nutrient poor waters on the AB. No correlations were observed between
 285 either PCs and the percentage contribution of the different groups to total biomass (Table 1).

286 **Table 1.** Results of Principal Component Analysis (PCA), including eigenvalues and Pearson
 287 correlation coefficients for the relationships between PC scores, hydrographic variables, and
 288 absolute and relative phytoplankton group biomass (n = 28). * $p < 0.05$; ** $p < 0.01$; *** $p <$
 289 0.005.

<i>Hydrography</i>	SST	\bar{E}_{SML}	N^2 max.	SML NO_3	SML $Si(OH)_4$
PC-1	-1.4 (-0.92***)	0.44 (0.29)	-0.39 (-0.26)	1.30 (0.85***)	1.06 (0.70***)
PC-2	-0.28 (-0.19)	-1.04 (-0.68***)	1.14 (0.75***)	-0.26 (-0.17)	0.79 (0.52**)
	PRO	SYN	PICO	NANO	CRYPTO
<i>Absolute Biomass</i>					
PC-1	-0.36	-0.41*	-0.45*	-0.27	-0.28
PC-2	-0.09	0.2	-0.004	-0.06	0.06
<i>Relative Biomass</i>					
PC-1	-0.02	-0.10	-0.1	0.29	-0.32
PC-2	-0.26	0.17	-0.07	0.03	0.16

291 4. Discussion

292 The average integrated biomass for the pico- and nanoplankton on the AB in autumn was 1.6
293 g C m^{-2} (range: 0.2 to 6.4 g C m^{-2}) which agrees well with a value of 1.9 g C m^{-2} for the global
294 ocean (Buitenhuis et al., 2012) and $\sim 2.2 \text{ g C m}^{-2}$ for similar regional shelf sea studies (e.g.,
295 Agusti et al., 2019; Wei et al., 2020; Chen et al., 2021). Overall, NANO showed the highest
296 contribution (average: 87%; range: 73 to 96%) to the total carbon biomass in surface, SCM
297 and integrated over the water column, with all other groups contributing less than 5%.
298 Dominance of phytoplankton biomass by nanoplankton agrees well with the size fractionated
299 pigment data from Poulton et al. (2022), highlighting higher contributions to total Chl of
300 nanoplankton than either pico- or microplankton.

301 On the east coast of South Africa, Barlow et al. (2002, 2020) reported elevated biomass and
302 a co-dominance between diatoms and haptophytes on the far eastern stations between 26.5
303 and 27.5 °E due to the upwelling of nutrient rich waters. This is indicative of the
304 nanoplankton dominance in the region upstream (east) of our sampling area. Lamont et al.
305 (2018) also highlighted nanoplankton as important to the AB despite showing a lower
306 contribution than microplankton. The nano-sized group has been observed to be more
307 prominent in warmer shelf waters, where they are able to take advantage of high nutrient
308 concentrations (Barlow et al., 2001, 2017).

309 Despite the highly stratified nature of the AB (Carter et al., 1987; Largier and Swart, 1987),
310 the distribution of pico- and nanoplankton biomass for the different groups showed no
311 strong vertical patterns (Figure 2). Though biomass of all groups was slightly higher in the
312 SCM, these differences were not statistically significant and the SCM did not represent a
313 strong biomass maximum as found in other shelf sea systems (e.g., Mena et al., 2019;
314 Barnett et al., 2019). During autumn on the AB, light availability in the SCM decreased
315 from east to west (Poulton et al., 2022), this is likely linked to peak biomass observed on
316 some stations on the west, and thus may have prevented strong biomass maxima forming at
317 depth. Previous studies on the central AB have observed SCM with considerable Chl
318 concentrations ($>10 \text{ mg m}^{-3}$) and phytoplankton biomass (Carter et al., 1987), though such
319 high Chl SCM were not observed during autumn in 2019.

320 While the AB had identifiable gradients in hydrographic conditions, as recognised in the PCA
321 (Table 1) and other related studies (Poulton et al., 2022; Noyon et al., 2022), there were few

322 clear relationships between phytoplankton group biomass or community composition. Only
323 PRO and SYN biomass correlated with PC1, indicating that these groups had higher biomass
324 in warmer, more nutrient impoverished waters, potentially linked to the offshore Agulhas
325 Current (Probyn et al., 1994; Jackson et al., 2012; Malan et al., 2018). This lack of linkage
326 between phytoplankton biomass and composition potentially relates to non-limiting nutrient
327 and light conditions (Poulton et al., 2022) across the section of the bank sampled in autumn
328 2019 (i.e., not near coast or off shelf waters).

329 Alternatively, nanoplankton dominance on the AB in autumn may be linked to the importance
330 of grazing in controlling community composition. Indeed, a strong link between NPP and
331 secondary production was observed in autumn 2019 (Noyon et al., 2022; Poulton et al.,
332 2022), and an importance of microzooplankton as active grazers and agents of trophic transfer
333 on the bank has been highlighted before (Huggett et al., 2023). Globally, ~64% of
334 phytoplankton daily primary production is grazed by micro-zooplankton, with the smaller
335 pico- and nanoplankton readily grazed by planktonic ciliates, heterotrophic flagellates, and
336 small zooplankton (Calbet and Landry, 2004; Mayers et al., 2019).

337 With the warming of the ocean, it is expected that the phytoplankton will shift from large-
338 species dominance to smaller nano-sized phytoplankton (Bopp et al., 2005; Lomas et al.,
339 2012; Dutkiewicz et al., 2013; Henson et al., 2021). This will in turn have a large impact on
340 the grazers, suggesting a decrease in food quality and a shift in the size structure of
341 zooplankton from large to smaller groups (Safi et al., 2023). Our study further highlights the
342 importance of microzooplankton on the AB in autumn, warranting further attention on these
343 organisms in supporting the ecosystems of the AB.

344 A shift in the global trends of phytoplankton size structure from large to smaller sized
345 phytoplankton has previously been observed and is projected in the future (Bopp et al., 2005;
346 Lomas et al., 2012; Dutkiewicz et al., 2013; Henson et al., 2021). This is mainly attributed to
347 the warming of the oceans and a depletion of nutrient supplies, giving advantage to the nano-
348 and picoplankton communities to flourish. The dominance of nanoplankton biomass on the
349 AB shelf ecosystem is comparable to other shelf regions. A similar shift in the community
350 from the larger phytoplankton to the smaller phytoplankton was also indicated by Huggett et
351 al. (2023). On the AB, where there has been a scarcity of in-situ sampling of the plankton
352 community, shifts in size structure may have severe implications for the ecosystems
353 supported by AB productivity and there is an urgent need for further studies.

354 **Author contributions**

355 **Conceptualization:** Sixolile L. Mazwane, Alex J. Poulton, Margaux Noyon. **Formal**
356 **analysis:** Sixolile L. Mazwane, Alex J. Poulton, Margaux Noyon, Emma Rocke.
357 **Investigation:** Sixolile L. Mazwane, Alex J. Poulton. **Methodology:** Sixolile L. Mazwane,
358 Alex J. Poulton, Margaux Noyon, Emma Rocke. **Writing – original draft:** Sixolile L.
359 Mazwane, Alex J. Poulton, Margaux Noyon. **Writing – review & editing:** Sixolile L.
360 Mazwane, Alex J. Poulton, Margaux Noyon, Emma Rocke. **Project administration and**
361 **Funding Acquisition:** Mike J. Roberts.

362 **Conflict of interest**

363 The authors declare no conflicts of interest relevant to this study.

364 **Data Availability Statement**

365 Chlorophyll, CTD and nutrient data from EK188 is available through the British
366 Oceanographic Data Centre (BODC) at doi:10.5285/d5cea266-fbec-7ef0-e053-6c86abc0722c.
367 Flow cytometry count data has been submitted to Zenodo and can be accessed at
368 <https://doi.org/10.5281/zenodo.10674482>.

369 **Acknowledgements**

370 We thank the captain and crew of the R/V *Ellen Khuzwayo*, together with the Department of
371 Forestry, Fisheries, and the Environment (DFFE). This study was produced with the
372 financial support of the Global Challenges Research Fund (GCRF), UK, in the framework of
373 the SOLSTICE-WIO project, under NERC grant NE/P021050/1. This work was also part of
374 the UK-SA bilateral chair Ocean Science and marine food security funded by the NRF/DST
375 Grant (98399) and the British Council grant SARCI150326116102. We thank the Health
376 Sciences department at the University of Cape Town (UCT) for the use of their Flow
377 Cytometer. We would like to thank the ESA Ocean Colour CCI project for processing and
378 providing the *Chl-a* dataset online at <http://www.esa-oceancolour-cci.org/>.

379 **References**

380 Acevedo-Trejos, E., Brandt, G., Bruggeman, J., & Merico, A. (2015). Mechanisms shaping
381 size structure and functional diversity of phytoplankton communities in the ocean.
382 Scientific Reports, 5, 17–20. <https://doi.org/10.1038/srep08918>

383 Agusti, S., Lubián, L.M., Moreno-Ostos, E., Estrada, M., & Duarte, C.M., 2019. Projected
384 Changes in Photosynthetic Picoplankton in a Warmer Subtropical Ocean. *Front. Mar.*
385 *Sci.* 5:506. doi: 10.3389/fmars.2018.00506

386 Barlow, R. G., Lamont, T., Kyewalyanga, M., Sessions, H., Morris, T., Carter, R. A., et al.
387 (2001). Chapter 6 : Latitudinal Changes in the Shape, Formation and Ecology of the
388 Chlorophyll a Maximum in the Subtropical and. *South African Journal of Marine*
389 *Science*, 54(1), 525–536. <https://doi.org/10.1016/j.rse.2017.09.038>

390 Barlow, R. G., Aiken, J., Holligan, P. M *Oceanographic Research Papers*, 49(4), 637–660.
391 [https://doi.org/10.1016/S0967-0637\(01\)00081-4](https://doi.org/10.1016/S0967-0637(01)00081-4)

392 Barlow, R., Lamont, T., Kyewalyanga, M., Sessions, H.,., Cummings, D. G., Maritorena, S.,
393 & Hooker, S. (2002). Phytoplankton pigment and absorption characteristics along
394 meridional transects in the Atlantic Ocean. *Deep-Sea Research Part I: & Morris, T.*
395 (2010). *Phytoplankton production and physiological adaptation* 30(13), 1472–
396 1486. <https://doi.org/10.1016/j.csr.2010.05.007>

397 Barlow, R., Lamont, T., Gibberd, M. J., Airs, R., Jacobs, L., & Britz, K. (2017).
398 Phytoplankton communities and acclimation in a cyclonic eddy in the southwest
399 Indian Ocean. *Deep-Sea Research Part I: Oceanographic Research*
400 *Papers*, 124, 18–30. <https://doi.org/10.1016/j.dsr.2017.03.013>

401 Barlow, R., Lamont, T., Gibberd, M. J., Russo, C., Airs, R., Tutt, G., et al. (2020).
402 Phytoplankton adaptation and absorption properties in an Agulhas Current ecosystem.
403 *Deep-Sea Research Part I: Oceanographic Research Papers*, 157(December 2019),
404 103209. <https://doi.org/10.1016/j.dsr.2019.103209>

405 Barnett, M.L., Kemp, A.E.S., Hickman, A.E. & Purdie, D.A. (2019). Shelf Sea subsurface
406 chlorophyll maximum thin layers have a distinct phytoplankton community structure.
407 *Continental Shelf Research*, Volume 174, 2019, 140-157,
408 <https://doi.org/10.1016/j.csr.2018.12.007>.

409 Becker, S., Aoyama, M., Woodward, E.M.S., Bakker, K., Coverly, S., Mahaffey, C., &
410 Tanhua, T.(2020). GO-SHIP repeat hydrography nutrient manual: the precise and
411 accurate determination of dissolved inorganic nutrients in seawater, using continuous
412 flow analysis methods. *Front. Mar. Sci.* 7, 581790.
413 <https://doi.org/10.3389/fmars.2020.581790>.

- 414 Bibby, T. S., & Moore, C. M. (2011). Silicate:nitrate ratios of upwelled waters control the
415 phytoplankton community sustained by mesoscale eddies in sub-tropical North
416 Atlantic and Pacific. *Biogeosciences*, 8(3), 657–666. [https://doi.org/10.5194/bg-8-657-](https://doi.org/10.5194/bg-8-657-2011)
417 2011
- 418 Bopp, L., Aumont, O., Cadule, P., Alvain, S., & Gehlen, M. (2005). Response of diatoms
419 distribution to global warming and potential implications: A global model study,
420 *Geophys. Res. Lett.*, 32, L19606, doi:10.1029/2005GL023653, 2005
- 421 Børsheim, K.Y., Bratbak, G. (1987). Cell volume to cell carbon conversion factors for a
422 bacterivorous *Monas* sp. enriched from seawater. *Mar. Ecol. Prog. Ser.* 36, 171–175.
- 423 Brzezinski, M.A. (1985). The Si:C:N ratio of marine diatoms: interspecific variability and
424 the effect of some environmental variables. *J. Phycol.* 21,
425 347–357. <https://doi.org/10.1111/j.0022-3646.198.00347.x>.
- 426 Buitenhuis, E.T., Li, W.K.W., Vaulot, D., Lomas, M.W., Landry, M.R., Partensky, F., Karl,
427 D.M., Ulloa, O., Campbell, L., Jacquet, S., Lantoine, F., Chavez, F., MacIas, D.,
428 Gosselin, M., McManus, G.B. (2012). Picophytoplankton biomass distribution in the
429 global ocean. *Earth Syst. Sci. Data* 4, 37–46. <https://doi.org/10.5194/essd-4-37-2012>
- 430 Calbet, A., & Landry, M. R. (2004). Phytoplankton growth, microzooplankton grazing, and
431 carbon cycling in marine systems. *Limnology and Oceanography*, 49(1), 51–57.
432 <https://doi.org/10.4319/lo.2004.49.1.0051>
- 433 Campbell, L. (2001). Flow Cytometric Analysis of Autotrophic Picoplankton, *Methods in*
434 *Microbiology*. Academic Press, pp. 317–343.
- 435 Carter, R. A., McMurray, H. F., Largier, J. L., McMurray, H. F., & Thermocline, J. L. L.
436 (1987). Thermocline characteristics and phytoplankton dynamics in Agulhas Bank
437 waters. *South African Journal of Marine Science*, 5(1), 327–336.
438 <https://doi.org/10.2989/025776187784522306>.
- 439 Carvalho, F., Kohut, J., Oliver, M.J. & Schofield, O. (2017). Defining the
440 ecologically relevant mixed-layer depth for Antarctica's coastal seas. *Geophys.*
441 *Res. Lett.* 44, 338–345. <https://doi.org/10.1002/2016GL071205>.

442 Chen, T.Y., Lai, C.C., Tai, J.H., Ko, C.Y., Shiah, F.K. (2021). Diel to Seasonal Variation of
443 Picoplankton in the Tropical South China Sea. *Front. Mar. Sci.* 8, 1–12.
444 <https://doi.org/10.3389/fmars.2021.732017>.

445 Chisholm, S. W., Olson, R. J., Zettler, E. R., Goericke, R., Waterbury, J. B. & Welschmeyer,
446 N. A. (1988). A novel free-living prochlorophyte abundant in the oceanic euphotic
447 zone. *Nature*, 334, 340–343.

448 Daneri, G., Lizárraga, L., Montero, P., González, H.E., Tapia, F.J. (2012). Wind forcing and
449 short-term variability of phytoplankton and heterotrophic bacterioplankton in the
450 coastal zone of the Concepcion upwelling system (Central Chile). *Prog. Ocea.*, 92-96.

451 Dutkiewicz, S., Scott, J. R. & Follows, M. J. (2013). Winners and losers: ecological and
452 biogeochemical changes in a warming ocean. *Glob. Biogeochem. Cycles* 27,
453 463-477.

454 Field, C. B., Behrenfeld, M. J., Randerson, J. T., & Falkowski, P. (1998). Primary production
455 of the biosphere: Integrating terrestrial and oceanic components. *Science*, 281(5374),
456 237–240. <https://doi.org/10.1126/science.281.5374.237>

457 Flander-Putrlle, V., Francé, J., & Mozetič, P. (2021). Phytoplankton pigments reveal size
458 structure and interannual variability of the coastal phytoplankton community (Adriatic
459 Sea). *Water (Switzerland)*, 14(1). <https://doi.org/10.3390/w14010023>

460 Flombaum, P., Wang, W.L., Primeau, F.W. et al. (2020). Global picophytoplankton niche
461 partitioning predicts overall positive response to ocean warming. *Nat. Geosci.* 13, 116–
462 120. <https://doi.org/10.1038/s41561-019-0524-2>

463 Henson, S.A., Cael, B.B., Allen, S.R. & Dutkiewicz, S. (2021). Future phytoplankton
464 diversity in a changing climate. *Nat Commun* 12, 5372.
465 <https://doi.org/10.1038/s41467-021-25699-w>

466 Huggett, J. A., Noyon, M., Carstensen, J., & Walker, D. R. (2023). Patterns in the plankton –
467 Spatial distribution and long-term variability of copepods on the Agulhas Bank. *Deep-
468 Sea Research Part II: Topical Studies in Oceanography*, 208,
469 105265. <https://doi.org/10.1016/j.dsr2.2023.105265>

470 Hutchings, L., van der Lingen, C.D., Shannon, L.J., Crawford, R.J.M., Verheye, H.M.S.,
471 Bartholomae, C.H., van der Plas, A.K., Louw, D., Kreiner, A., Ostrowski, M., Fidel,

472 Q., Barlow, R.G., Lamont, T., Coetzee, J., Shillington, F., Veitch, J., Currie, J.C., &
473 Monteiro, P.M.S. (2009). The Benguela Current: an ecosystem of four components.
474 *Prog. Oceanogr.* 83, 15–32. <http://dx.doi.org/10.1016/j.pocean.2009.07.046>.

475 Hydes, D. J., Aoyama, M., Aminot, A., Bakker, K., Becker, S., Coverly, S., et al. (2010).
476 Determination of dissolved nutrients (N, P, Si) in seawater with high precision and
477 inter-comparability using gas-segmented continuous flow analysers, In: *The GO-SHIP*
478 *repeat hydrography manual: A collection of expert reports and guidelines*. IOCCP
479 report No. 14. ICPO publication series No. 134.

480 Jackson, J. M., Rainville, L., Roberts, M. J., McQuaid, C. D., & Lutjeharms, J. R. E. (2012).
481 Mesoscale bio-physical interactions between the Agulhas Current and the Agulhas
482 Bank, South Africa. *Continental Shelf Research*, 49,
483 10–24. <https://doi.org/10.1016/j.csr.2012.09.005>

484 Lamont, T., Brewin, R. J. W., & Barlow, R. G. (2018). Seasonal variation in remotely-sensed
485 phytoplankton size structure around southern Africa. *Remote Sensing of Environment*,
486 204, 617–631. <https://doi.org/10.1016/j.rse.2017.09.038>

487 Liang, Y., Zhang, Y., Zhang, Y., Luo, T., Rivkin, R. B. and Jiao, N. (2017). Distributions and
488 relationships of virio- and picoplankton in the epi-, meso- and bathypelagic zones of
489 the Western Pacific Ocean. *FEMS Microbiology Ecology* 93(2), fiw238

490 Liu, H., Probert, I., Uitz, J., Claustre, H., Aris-Brosou, S., Frada, M., et al. (2009). Extreme
491 diversity in noncalcifying haptophytes explains a major pigment paradox in open
492 oceans. *Proceedings of the National Academy of Sciences of the United States of*
493 *America*, 106(31), 12803–12808. <https://doi.org/10.1073/pnas.0905841106>

494 Lomas, M. W., Moran, S. B., Casey, J. R., Bell, D. W., Tiahlo, M., Whitefield, J., et al.
495 (2012). Spatial and seasonal variability of primary production on the Eastern Bering
496 Sea shelf. *Deep-Sea Research Part II: Topical Studies in Oceanography*, 65–70,
497 126–140. <https://doi.org/10.1016/j.dsr2.2012.02.010>

498 Malan, N., Backeberg, B., Biastoch, A., Durgadoo, J. V., Samuelsen, A., Reason, C., &
499 Hermes, J. (2018). Agulhas Current meanders facilitate shelf-slope exchange on the
500 Eastern Agulhas Bank. *Journal Geophysical Research: Oceans*, 123, 4762–4778.
501 <https://doi.org/10.1029/2017JC013602>

502 Marañón, E. (2015). Cell size as a key determinant of phytoplankton metabolism and
503 community structure. *Ann Rev Mar Sci.* 7:241-64. doi: 10.1146/annurev-marine-
504 010814- 015955. Epub 2014 Jul 25. PMID: 25062405.

505 Marie, D., Partensky, F., Jacquet, S., Vaultot, D. (1997). Enumeration and cell cycle analysis
506 of natural populations of marine picoplankton by flow cytometry using the nucleic
507 acid stain SYBR Green I. *Appl. Environ. Microbiol.* 63, 186–193.

508 Mayers, K. M. J., Poulton, A. J., Daniels, C. J., Wells, S. R., Woodward, E. M. S., Tarran, G.
509 A., et al. (2019). Growth and mortality of coccolithophores during spring in a
510 temperate Shelf Sea (Celtic Sea, April 2015). *Progress in Oceanography*, 177,
511 101928. <https://doi.org/10.1016/j.pocean.2018.02.024>

512 Mazwane, S. L., Poulton, A. J., Hickman, A. E., Jebri, F., Jacobs, Z., Roberts, M., & Noyon,
513 M. (2022). Spatial and temporal variability of Net Primary Production on the Agulhas
514 Bank, 1998–2018. *Deep-Sea Research Part II: Topical Studies in Oceanography*, 199,
515 105079. <https://doi.org/10.1016/j.dsr2.2022.105079>

516 Mena, C., Reglero, P., Hidalgo, M., Sintes, E., Santiago, R., Martín, M., Moyà, G. & Balbín,
517 R. (2019). Phytoplankton Community Structure Is Driven by Stratification in the
518 Oligotrophic Mediterranean Sea. *Front. Microbiol.* 10:1698.
519 doi:10.3389/fmicb.2019.01698

520 Mitra, A., Caron, D.A., Faure, E., Flynn, K.J., Gonçalves Leles, S., Hansen, P.J. et al. (2023).
521 The Mixoplankton database (MDB). Zenodo. <https://doi.org/10.5281/zenodo.7560583>

522 Moore, C. M., Suggett, D., Holligan, P. M., Sharples, J., Abraham, E. R., Lucas, M. I., et al.
523 (2003). Physical controls on phytoplankton physiology and production at a shelf sea
524 front: A fast repetition-rate fluorometer based field study. *Marine Ecology Progress*
525 *Series*, 259, 29–45. <https://doi.org/10.3354/meps259029>

526 Moore, C.M., Mills, M.M., Achterberg, E.P., Geider, R.J., LaRoche, J., Lucas, M.I.,
527 McDonagh, E.L., Pan, X., Poulton, A.J., Rijkenberg, M.J.A., Suggett, D.J., Ussher, S.
528 J. & Woodward, E.M.S. (2009). Large-scale distribution of Atlantic nitrogen
529 fixation controlled by iron availability. *Nat. Geosci.* 2, 867–871.
530 <https://doi.org/10.1038/ngeo667>.

531 Moran, M. A., 2015. The global ocean microbiome. *Science*.350(6225), aac8455.

- 532 Noyon, M. (2019). Oceanographic Survey of the Eastern and Central Agulhas Bank (South
533 Africa). Port Elizabeth.
- 534 Noyon, M., Poulton, A.J., Asdar, S., Weitz, R., Giering, S.L.C. (2022). Mesozooplankton
535 community distribution on the Agulhas Bank in autumn: Size structure and production.
536 Deep. Res. Part II Top. Stud. Oceanogr. 195,
537 105015. <https://doi.org/10.1016/j.dsr2.2021.105015>
- 538 Pauly, D., Christensen, V., Guénette, S., Pitcher, T. J., Sumaila, U. R., Walters, C. J., et al.
539 (2002). Towards sustainability in world fisheries. *Nature*, 418 (6898), 689–695.
540 <https://doi.org/10.1038/nature01017>
- 541 Poulton, A. J., Mazwane, S. L., Godfrey, B., Carvalho, F., Mawji, E., Wihsgott, J. U., &
542 Noyon, M. (2022). Primary production dynamics on the Agulhas Bank in autumn.
543 Deep-Sea Research Part II: Topical Studies in
544 Oceanography, 203. <https://doi.org/10.1016/j.dsr2.2022.105153>
- 545 Poulton, A. J., Young, J. R., Bates, N. R., & Balch, W. M. (2011). Biometry of detached
546 *Emiliania huxleyi* coccoliths along the Patagonian Shelf. *Marine Ecology Progress*
547 *Series*, 443, 1–17. <https://doi.org/10.3354/meps09445>
- 548 Probyn, T. A., Mitchell-Innes, B. A., Brown, P. C., Hutchings, L., & Carter, R. A. (1994). A
549 review of primary production and related processes on the Agulhas Bank. *South*
550 *African Journal of Science*, 90, 166–173.
- 551 Rajaneesh, K. M., Mitbavkar, S., Anil, A. C., & Sawant, S. S. (2015). *Synechococcus* as an
552 indicator of trophic status in the Cochin backwaters, west coast of India. *Ecological*
553 *Indicators*, 55, 118-130.
- 554 Rajaneesh, K. M., Mitbavkar, S., & Anil, A. C. (2017). Influence of short-term hydrographic
555 variations during the north-east monsoon on picophytoplankton community structure
556 in the eastern Arabian Sea. *Continental Shelf Research*, 146, 28–36.
557 <https://doi.org/10.1016/j.csr.2017.08.008>
- 558 Redfield, A.C. (1958). The biological control of chemical factors in the environment. *Am.*
559 *Sci.* 46, 205–221. <https://www.jstor.org/stable/27827150>.
- 560 Safi, K. A., Rodríguez, A. G., Hall, J. A., & Pinkerton, M. H. (2023). Phytoplankton
561 dynamics, growth and microzooplankton grazing across the subtropical frontal zone,

562 east of New Zealand. *Deep-Sea Research Part II: Topical Studies in Oceanography*,
563 208(January). <https://doi.org/10.1016/j.dsr2.2023.105271>

564 Scanlan D.J., Ostrowski, M., Mazard, S., Dufresne, A., Garczarek, L., Hess, W.R., Post, A.F.,
565 Hagemann, M., Paulsen, I., Partensky F. (2009). Ecological genomics of marine
566 picocyanobacteria; *Microbiology and molecular biology reviews* 73(2), 249-299

567 Sieburth, J. (1979). *Sea microbes*. Oxford University Press New York

568 Sonnekus, M.J. (2020). *Phytoplankton of the Southern Agulhas Large Marine Ecosystem*
569 (sACLME). PhD Thesis, Nelson Mandela University, Gqeberha (formerly Port
570 Elizabeth), South Africa. Pp1-262

571 Tarran, G. A., Heywood, J. L., & Zubkov, M. V. (2006). Latitudinal changes in the standing
572 stocks of nano- and picoeukaryotic phytoplankton in the Atlantic Ocean. *Deep-Sea*
573 *Research Part II: Topical Studies in Oceanography*, 53(14–16), 1516–1529.
574 <https://doi.org/10.1016/j.dsr2.2006.05.004>

575 Van Dongen-Vogels, V., Seymour, J.R., Middleton, J.F., Mitchell, J.G., Seuront, L. (2012).
576 Shifts in picophytoplankton community structure influenced by changing upwelling
577 conditions. *Estuar. Coast. Shelf Sci.* 109, 81–90.
578 <https://doi.org/10.1016/j.ecss.2012.05.026>

579 Van Dongen-Vogels, V., Seymour, J.R., Middleton, J.F., Mitchell, J.G., Seuront, L. (2011).
580 Influence of local physical events on picophytoplankton spatial and temporal dynamics
581 in South Australian continental shelf waters. *J. Plankton Res.* 33, 1825–
582 1841. <https://doi.org/10.1093/plankt/fbr077>

583 Wang, F., Wei, Y., Zhang, G., Zhang, L., & Sun, J. (2022). Picophytoplankton in the West
584 Pacific Ocean: A Snapshot. *Frontiers in Microbiology*, 13, 1–13.
585 <https://doi.org/10.3389/fmicb.2022.811227>

586 Waterbury, J. B., Watson, S. W., Guillard, R. R. L. et al. (1979) Widespread occurrence of a
587 unicellular, marine planktonic, cyano- bacterium. *Nature*, 277, 293–294. Wei, Y.,
588 Huang, D., Zhang, G., Zhao, Y. & Sun, J. (2020). Biogeographic variations of
589 picophytoplankton in three contrasting seas: The Bay of Bengal, South China Sea and
590 western Pacific Ocean. *Aquat. Microb. Ecol.* 84, 91–103.
591 <https://doi.org/10.3354/ame01928>

- 592 Wei, Y., Huang, D., Zhang, G., Zhao, Y., & Sun, J. (2020). Biogeographic variations of
593 picophytoplankton in three contrasting seas: The Bay of Bengal, South China Sea and
594 western Pacific Ocean. *Aquatic Microbial Ecology*, 84(1), 91–
595 103. <https://doi.org/10.3354/ame01928>
- 596 Worden, A. Z. (2006). Picoeukaryote diversity in coastal waters of the Pacific Ocean.
597 *Aquatic Microbial Ecology*, 43(2), 165-175.